IMPERIAL COLLEGE LONDON

Department of Earth Science and Engineering

Centre for Petroleum Studies

The Viscosity of Asphaltene- Containing Oil

By

Oluwateleola O. Odubanjo

A thesis submitted in partial fulfilment of the requirements for the MSc degree and/or the DIC.

September 2011

DECLARATION OF OWN WORK

I declare that this thesis *The Viscosity of Asphaltene – Containing Oil* is entirely my own work and that where any material could be construed as the work of others, it is fully cited and referenced, and/ or with appropriate acknowledgement given.

Signature:

Name of Student: Oluwateleola O. Odubanjo
Names of Supervisors: Dr. Velisa Vesovic, Dr. Nicolas Riesco, Kazeem A. Lawal

Abstract

This study takes advantage of experimental data sets to develop a simple empirical model for the prediction of heavy oil viscosity, using the viscosity of maltene, temperature, and asphaltene weight fraction as input data.

Given the viscosity measurements of reconstituted Lloydminster heavy oil samples, with asphaltene weight fractions within the range 0 to 0.1601 wt/wt (Luo *et al.*, 2007), the colloidal viscosity models of Brady (1993), Verberg *et al.* (1997) and Einstein (1906) are employed to determine the variations between the effective asphaltene volume fraction and the dry asphaltene volume fraction, calculated according to Luo *et al.* (2007). Of the three models, both Brady (1993) and Verberg *et al.* (1997) show the most consistent results, with values of effective asphaltene volume fraction closely tracking each other, and of the same order of magnitude, though considerably larger than the dry asphaltene volume fractions. The Einstein (1906) model proves to be applicable only at very low asphaltene weight fractions, and is disregarded for most part of the study.

To rationalise the disparity between the effective and dry asphaltene volume fractions, a steric structural model for the solvation of asphaltenes is explored. The model assumes asphaltene particles become colloidal dispersions in oil due to the presence of resins and other polar molecules, which adsorb onto the surface of the asphaltene particles, thereby increasing its overall effective volume fraction. This model results in an equation that gives the effective volume fraction as a function of the asphaltene weight fraction, the asphaltene particle radius, and the resin shell thickness.

With the effective volume fraction, the viscosities of the reconstituted heavy oil samples can then be determined using either Brady (1993) or Verberg *et al.* (1997) models. The results are compared with measured experimental data and are found to be in reasonable agreement, showing deviations within a ±5% error margin from the measured experimental data.

Acknowledgements

It is my pleasure to acknowledge all the people who have made this thesis possible. Firstly, I would like to show my gratitude to Dr. Velisa Vesovic for providing me with the invaluable opportunity to work with himself and his team on this project- for his good teachings, insightful criticism and support. I owe my deepest gratitude to Dr. Nicolas Riesco, for his great ideas, direction, guidance and ceaseless support for the entire duration of the project. I would also like to thank Kazeem A. Lawal, also for his continuous support and for his delightful enthusiasm throughout this period- to my supervisors, I am truly grateful. I would also to express my gratitude to Prof. Yongan Gu of the University of Regina who provided the experimental data set used throughout this study.

I am forever grateful to my family and especially my mother, to whom I dedicate this thesis, for her ceaseless love, concern and encouragement.

I owe my deepest gratitude to my Father, for His blessings of wisdom, strength and grace for growth, throughout what has been a very challenging year.

Table of Contents

List of Figures

List of Tables

The Viscosity of Asphaltene – Containing Oil

Oluwateleola O. Odubanjo

Imperial College London

V. Vesovic, N. Riesco, and K. A. Lawal, Imperial College London

Abstract

This study takes advantage of experimental data sets to develop a simple empirical model for the prediction of heavy oil viscosity, using the viscosity of maltene, temperature, and asphaltene weight fraction as input data.

Given the viscosity measurements of reconstituted Lloydminster heavy oil samples, with asphaltene weight fractions within the range 0 to 0.1601 wt/wt (Luo *et al.*, 2007), the colloidal viscosity models of Brady (1993), Verberg *et al.* (1997) and Einstein (1906) are employed to determine the variations between the effective asphaltene volume fraction and the dry asphaltene volume fraction, calculated according to Luo *et al.* (2007). Of the three models, both Brady (1993) and Verberg *et al.* (1997) show the most consistent results, with values of effective asphaltene volume fraction closely tracking each other, and of the same order of magnitude, though considerably larger than the dry asphaltene volume fractions. The Einstein (1906) model proves to be applicable only at very low asphaltene weight fractions, and is disregarded for most part of the study.

To rationalise the disparity between the effective and dry asphaltene volume fractions, a steric structural model for the solvation of asphaltenes is explored. The model assumes asphaltene particles become colloidal dispersions in oil due to the presence of resins and other polar molecules, which adsorb onto the surface of the asphaltene particles, thereby increasing its overall effective volume fraction. This model results in an equation that gives the effective volume fraction as a function of the asphaltene weight fraction, the asphaltene particle radius, and the resin shell thickness.

With the effective volume fraction, the viscosities of the reconstituted heavy oil samples can then be determined using either Brady (1993) or Verberg *et al.* (1997) models. The results are compared with measured experimental data and are found to be in reasonable agreement, showing deviations within a ±5% error margin from the measured experimental data.

Introduction and Background

The growing focus and demand for unconventional heavy oils, and bitumen is the results of the gradual depletion of conventional light and medium oil resources coupled with a steadily increasing demand for energy worldwide.
Heavy oil and bitumen resources are characterised by their high viscosities (i.e. >100 mPa.s for heavy oil and >10 000 mPa.s for bituminous reserves) and low API gravities (i.e. <22.3°API for heavy oil and <10°API for bitumen) (Speight, 1991). These properties are not only the result of high molecular weight hydrocarbons but also importantly, of high asphaltene contents (i.e. up to 50 wt %) in some heavy oils (Luo *et al.*, 2007). Asphaltenes are defined as the component of petroleum liquids that represent the most refractory (or heaviest) fraction of the petroleum hydrocarbons (Sheu *et al.*, 1995). In terms of solvent solubility, asphaltene is defined as petroleum component that is insoluble in n-alkanes including n-pentane or n-heptane, but soluble in toluene.

Heavy oil and bitumen deposits exist in vast amounts around the world, with the deposits of the USA, western Canada, Mexico, and the Middle East, remaining some of the most popular. The total World oil resources currently lie between 9 and 13 trillion barrels of which a significant 40% are heavy and extra heavy oils, with another 30% consisting of oil sands and bitumen (Schlumberger, 2011). Approximately 19 billion barrels of viscous, heavy oil are located in the Lloydminster area, Canada, where recovery factors after cold production are in the range of 8% to 15% OOIP (Alvares *et al.*, 2009). Canadian oil sands with higher viscosities can be impossible to produce at all by primary methods and are usually immediately produced with steam injection. Thus, accurate estimates of heavy oil viscosities would prove not only crucial for cost effective upstream recovery, but also for effective downstream transportation and improved refining technologies.

Several factors contribute to difficulties in the reliable prediction of the viscosity of heavy oils. The complex nature of heavy oil, largely the result of the presence of asphaltenes, waxes, scales and other heavy and complex components, does not allow for the reliable viscosity predictions. Temperature changes during sample retrieval, transportation and storage strongly affect the viscosity of the sample. According to de la Porte *et al.* (2009), it is not uncommon for an increase in temperature of ten of degrees to reduce the viscosity by 2 to 3 orders of magnitude. Other important factors including the formation of heavy oil/ connate water emulsions during extraction, blending with light components and sample contamination also lead to considerable errors in the viscosity of heavy oil. Based on studies of reservoir sensitivity of reservoir simulations to uncertainties in viscosity, Hernandez *et al.* (2002) found that for heavy oils ($\mu > 6$ cp), a ±10% error in viscosity will propagate

an error in cumulative production of approximately ±10% in most heterogeneous reservoirs studied.

Over the years, the dependence of the viscosity of heavy oil on the volume fraction, chemical structures and physiochemical properties of the asphaltenes present in the oil has been greatly emphasised: Mack (1932) showed through his studies of Mexican asphalts that reconstituted oil with 20 vol% of asphaltenes had a viscosity 367 times higher than that of maltene (i.e. oil with a 0 vol% asphaltene content). Dealy (1979) based his studies of the effect of asphaltene concentration on the viscosity of Athabasca bitumen, showing that an additional 5 wt% asphaltenes into the original sample, increases its viscosity from 300 000 to 1 000 000 mPa.s. Hirschberg (1984) found that the viscosity of a North African oil sample increased from 9 to 36 mPa.s when the asphalt content increased from 10 to 16%.

Since its proposal by Nellensteyn (1931), asphaltenes in oil have been best modelled as a colloidal suspension system. However, it was not until the detailed work of Pfeiffer and Saal (1940), that the model became accepted (Sheu *et al.*, 1995). Pfeiffer *et al.* (1940) produced a model for a asphaltene/ maltene/ resin complex, where asphaltenes are assumed to be solvated in the oil by non-asphaltenic molecules (resins) to form what is still known today as 'micelles'. Several theoretical models and empirical correlations based on this colloidal suspension model have been used to determine the viscosity of asphaltene-containing oil, with the results found to be most influenced by the volume fraction and solvation effects of the asphaltene particles, and the intrinsic viscosity.

Existing Colloidal Suspension Viscosity Models. Einstein (1906) instigated the modelling of a dilute dispersion with the equation below:

$$\mu_r = \frac{\mu}{\mu_o} = 1 + 2.5\varphi \tag{1}$$

where μ_r is the relative viscosity of the colloidal suspension, defined as the ratio of the viscosity of the colloidal dispersion, μ to the viscosity of the continuous phase, μ_o, and φ is the asphaltene volume fraction. The constant *2.5*, in the equation above, is representative of the shape factor, ν, suggesting rigid spherical particles with zero solvation effect so that *K*=1.

Several other equations have been proposed in literature for the viscosity of Newtonian systems. Sherman (1983) describes the viscosity versus concentration behaviour of Newtonian emulsions using the equation:

$$\mu_r = 1 + a\varphi + b\varphi^2 + c\varphi^3 + \cdots \tag{2}$$

where the constants *a*, *b* and *c* etc. differ with emulsion systems. As these constants are all unknown variables, the equation can only be used to make correlations where there is specific viscosity data and can not be used to predict the viscosity of emulsions.

Pal and Rhodes (1989) proposed the following equation for an emulsion with spherical droplets (i.e. ν=2.5) and a dispersed phase with a dry volume fraction greater than 10%:

$$\mu_r = (1 - K\varphi)^{-2.5} \tag{3}$$

In the case of non-spherical particles, the above equation can be generalised to give:

$$\mu_r = (1 - K\varphi)^{-\nu} \tag{4}$$

where ν, again represents the shape factor of the solid particles.

Mooney (1951) developed an equation to account for cases where solid particles or liquid droplets in an emulsion are densely dispersed so that there is not enough space to move around. In such cases, the volume fraction of the dispersed solid particles or liquid droplets is less than unity, and the viscosity of such colloidal dispersions approaches infinity. This is known as the maximum packing volume fraction φ_{max}. The semi-empirical equation is expressed as:

$$\mu_r = exp\left[\frac{[\mu]\varphi}{1-\frac{\varphi}{\varphi_{max}}}\right] \tag{5}$$

where $[\mu]$ is the intrinsic viscosity.

In 1993, Brady developed a simple model for the rheological behaviour of concentrated colloidal dispersions. For a suspension of Brownian hard spheres, he assumed two contributions to the macroscopic stress: a hydrodynamic and Brownian stress. The

hydrodynamic stress results in the high-frequency dynamic viscosity with the Brownian stress responsible for the viscoelastic behaviour of the colloidal dispersion (Brady, 1993). Brady's theory predicts that viscosity diverges as the colloidal volume fraction approaches the close packing volume fraction, or φ_{max} as the number of 'contacting' particles becomes infinite due to the presence of hydrodynamic forces causing the contacting particles to stick together (Brady, 1993). Verberg *et al*. (1997) developed a theoretical formula for the Newtonian viscosity of colloidal suspensions. The expression is a linearised solution of the Smoluchowski equation, using a Padé approximation of the viscosity of the solution, $\mu(\varphi)$ that can be conveniently used for all volume fractions within the range $0<\varphi<0.55$, providing results within a relative accuracy of less than 0.25%.
Also in 1997, Hiemenz *et al*. produced a more rigorous version of Sherman's equation (eq. 2), where the relative viscosity of a colloidal dispersion is expressed as:

$$\mu_r = 1 + \nu\varphi_{eff} + k_1\varphi_{eff}^2 + k_2\varphi_{eff}^3 + \cdots \tag{6}$$

where φ_{eff} symbolises the effective volume fraction of the dispersed phase in the colloidal dispersion after solvation effects have taken place, and k_1 and k_2 are both coefficients.

If φ is defined as the dry volume fraction of the dispersed phase before dispersion, then the solvation constant, *K*, can be defined as:

$$K = \frac{\varphi_{eff}}{\varphi} \tag{7}$$

Eq. 6 can then be rearranged to give:

$$\mu_r = \frac{\mu}{\mu_o} = 1 + [\mu]\varphi + K_1\varphi^2 + K_2\varphi^3 + \cdots, \tag{8}$$

where the intrinsic viscosity, $[\mu]$ now represents the joint effects of shape factor and solvation:

$$[\mu] = K\nu \tag{9}$$

Luo *et al.* (2007) used the Arrhenius equation to examine the effect of temperature on the viscosity of a heavy oil sample with the same asphaltene volume fraction but at different temperatures:

$$\mu(T) = \mu(T_o)\exp\left[\frac{E_a}{R}\left(\frac{1}{T} - \frac{1}{T_o}\right)\right] \tag{10}$$

where $\mu(T)$ is the liquid viscosity at the absolute temperature, T; $\mu(T_o)$ is the liquid viscosity at a reference temperature, T_o; E_a is the activation enthalpy of viscous flow (J/mol); and R, the universal gas constant (J/K mol).

Luo *et al.* (2007) found that heavy oils with high asphaltene content have greatly increased viscosities as a result of strong interactions among the asphaltene molecules. At increased temperature, it is found that even heavy oil with high asphaltene content, has a significantly reduced viscosity, due to increased molecular thermal energy, allowing liquid molecules overcome energy barriers and move into nearby vacant sites (Luo *et al.*, 2007). Based on a computational scheme for a two-parameter search using the Pal- Rhodes equation (eq. 4), Luo *et al.* (2007) found solvation constants, $K>1$, indicating noticeable solvation, with steric resin layers forming around the asphaltene molecules. At higher temperatures, lower solvation constants suggest de-adsorption of resins at the outermost layers as the molecules gain enough thermal energy to escape from the surface asphaltene particles.

The aim of this study is to take advantage of experimental data to develop a simple model for the prediction of heavy oil viscosity as a function of the viscosity of maltene, μ_0 temperature, T and asphaltene weight fraction, ω, within an experimental accuracy of 5%.

Methodology

Experimental Data. The heavy oil sample used in this study is provided by Luo *et al.* (2007). The sample was taken from the Lloydminster area, Canada, which forms part of the Western Canadian Sedimentary Basin, *WCSB*. Compositional analysis of the original oil field sample indicated the absence of light components between and including C_1 to C_{11} and almost half of the components (wt%=47.50) were found to be C_{50+}. The asphaltene content of the original sample, ω_{asp}, was 14.50 wt% (n-pentane insoluble). The density and viscosity of the cleaned field oil sample were reported to be ρ_o= 988 kg/m^3 and μ_o= 24 137 mPa.s at atmospheric pressure and 23.9°C, respectively (Luo *et al.*, 2007).

As reported by Luo *et al.* (2007) the original oil field sample was converted first into a deasphalted heavy oil sample by implementing the standard ASTM D2007 method. The density of the deasphalted heavy oil, or maltene, was reported to be 962 kg/m^3 at atmospheric pressure and 23.9°C. The asphaltenes extracted were added at different asphaltene content into the maltene and its viscosity measured at atmospheric pressure. The reconstitution process used ten different asphaltene contents with a weight fraction, ω within the range 0 to 16.01 wt%, at six different temperatures, T within 293.15 to 333.15K (20.0 to 60.0°C), to give a total of 66 samples (including the deasphalted heavy oil sample) with viscosities in the range of μ= 118.7 to 53 672 mPa.s.
Luo *et al.* (2007) determine an asphaltene volume fraction within the range, φ= 0 to 13.50 vol%, based on the expression below:

$$\varphi = \frac{\rho_o}{\rho_a}\omega \tag{11}$$

where ρ_a is the density of asphaltene, estimated from the equation below:

$$\rho_a = \frac{\omega_{asp}}{\frac{1}{\rho_o} - \frac{1-\omega_{asp}}{\rho_m}} \tag{12}$$

The density of asphaltene, ρ_a was found to be 1175.3 kg/m^3, while, ω_{asp}= 16.01 wt%, ρ_o= 988 kg/m^3 and ρ_m= 962 kg/m^3.

Density Approach for the Determining Dry Volume Fraction, φ. According to Luo et al. (2007), eq. (11) for calculating asphaltene volume fraction, φ, assumes the density of the oil sample, ρ_o to be constant across all isotherms. This approach however, coupled with Aasen et al. (1990) method for the density of the hydrocarbon mixture (described later in this section) allows for the determination of the dry asphaltene volume fractions as a function of temperature. Assuming the oil is a binary mixture consisting of asphaltene and maltene, to a large extent, the change in density of asphaltene is considered negligible, as it is a solid, however the density of the maltene, as a liquid should vary with temperature.

The model described below expresses asphaltene volume fraction, φ in terms of its weight fraction, ω, whilst taking into account changing the density of maltene.

For an ideal binary mixture of asphaltene and maltene:

$$V_o = V_a + V_m \tag{13}$$

where V_o= volume of the oil sample, V_a= volume of asphaltene and V_m= volume of maltene.

The dry volume fraction of asphaltene is defined as:

$$\varphi = \frac{V_a}{V_a + V_m} \tag{14}$$

Volume can be expressed in terms of densities, ρ and masses, m, of the different components, such that:

$$V_a = \frac{m_a}{\rho_a} \tag{15}$$

$$V_m = \frac{m_m}{\rho_m} \tag{16}$$

where m_a= mass of asphaltene, m_m= mass of maltene, ρ_a= density of asphaltene, and ρ_m= density of maltene.

Substituting equations (15) and (16) into eq. (14):

$$\varphi = \frac{\frac{m_a}{\rho_a}}{\frac{m_a}{\rho_a} + \frac{m_m}{\rho_m}} \tag{17}$$

$$\varphi = \frac{m_a}{m_a + \frac{\rho_a}{\rho_m} m_m} \tag{18}$$

Component masses may be expressed in terms of weight fractions:

$$\omega_a = \frac{m_a}{m_a+m_m} \quad (19)$$

$$\omega_m = \frac{m_m}{m_a+m_m} \quad (20)$$

where ω_m= weight fraction of maltene

$$\omega_a+\omega_m = 1 \quad (21a)$$

$$\omega_m = 1- \omega_a \quad (21b)$$

Let:

$$m_a+m_m = m_o \quad (22)$$

where m_o= mass of oil

Therefore,

$$m_a = \omega_a m_o \quad (23)$$

$$m_m = (1-\omega_a)m_o \quad (24)$$

Substituting eq. (23) and (24) into eq. (18) yields:

$$\varphi = \frac{\omega_a m_o}{\omega_a m_o+\frac{\rho_a}{\rho_m}(1-\omega_a)m_o} \quad (25)$$

In terms of only asphaltene weight fraction, ω_a:

$$\varphi = \frac{\omega_a}{\omega_a+\frac{\rho_a}{\rho_m}(1-\omega_a)} \quad (26)$$

The density of the maltene, ρ_m is then approximated as the density of a hydrocarbon as described by Aasen *et al.* (1990).

According to Li *et al.* (1956) the density of the hydrocarbon mixture at 298.15K, assuming the mixture is an n-alkane is:

$$\rho(T = 298K) = \frac{M}{V_0+an+\frac{b}{n-1}+\frac{c}{(n-1)^2}} \quad (27)$$

where, *ρ(T= 298K)* is the density of the n-alkane at 298K (g/cm^3), *M* is the molecular weight (g/mol), V_0= 45.822 33 cm^3/mol, *a*= 16.4867 cm^3/mol, *b*= 14.563 29 cm^3/mol, *c*= -4.56336 cm^3/mol, and *n* is the number of carbons per molecule.

The corresponding coefficient of thermal expansion is taken from Kartsev *et al.* (1997)

$$\alpha = \alpha_0 \exp(\beta/n) \quad (28)$$

where α_0= 6.7776×10^{-4} K^{-1} and β= 4.2541.

A combination yields the desired equation:

$$\rho = \rho(T= 298K)(1- \alpha(T- 298)) \quad (29)$$

Colloidal Suspension Viscosity Models. For the purpose of this study, three models used in determining the viscosity of colloidal suspensions will be tested as the foundation of the model build for the prediction of heavy oil viscosity; these are the Einstein (1906) (eq. 1), Brady (1993), and Verberg *et al.* (1997) models.

Brady (1993). Brady developed a simple expression for the rheological behaviour for the concentrated colloidal suspension of Brownian hard spheres for which he assumed two contributions to the macroscopic stress: a hydrodynamic and Brownian stress. The hydrodynamic stress results in the high-frequency dynamic viscosity, while the latter is responsible for the viscoelastic behaviour of the colloidal dispersion (Brady, 1993).

$$\frac{\mu}{\mu_0} = \left(1 - \frac{\varphi}{0.63}\right)^{-2} \tag{30}$$

where 0.63 is representative of φ_{max}, the maximum packing fraction for hard spheres (Heyes et al., 2004).

Brady's theory predicts that viscosity diverges as the colloidal volume fraction approaches φ_{max} as the number of 'contacting' particles becomes infinite and short time self- diffusivity becomes negligible due to the presence of hydrodynamic forces causing the contacting particles to stick together (Brady, 1993).

Verberg et al. (1997). The theoretical formula for the Newtonian viscosity of colloidal suspensions is expressed:

$$\mu(\varphi) = \mu_0 \chi(\varphi)\left[1 + \frac{1.44\varphi\chi(\varphi)^2}{1-0.1241\varphi+10.46\varphi^2}\right] \tag{31}$$

The term $\chi(\varphi)$ is defined using the Carnahan- Starling approximation describing the radial distribution for a hard- sphere fluid suspension:

$$\chi(\varphi) = \frac{1-0.5\varphi}{(1-\varphi)^3} \tag{32}$$

Model Validation. The colloidal suspension viscosity models were validated by substituting the measured viscosities of the reconstituted heavy oil samples, μ and the viscosity of the maltene samples, μ_0 (i.e. ω=0 wt%) across all six isotherms, as a back- calculation, in order to determine the effective volume fractions, φ_{eff}, and then compare the values with the dry volume fractions calculated according to Luo *et al.* (2007), with eq. (11).

Solvation Shell Model. It is generally understood that asphaltene molecules become colloidal dispersions in oil due to the presence of polar molecules, aromatics and resins. Resins are defined as the fraction of crude oil soluble in light alkanes such as pentane and heptane, but insoluble in liquid propane (Speight, 1999). Though they form part of the oil phase, resins have a higher polarity than that of gas oil (saturates and aromatics), allowing the molecules to be easily adsorbed to the surface of the asphaltene aggregates (Aske *et al.*, 2002). This adsorption is responsible for keeping asphaltene dispersed in the crude oil. Analysis techniques including X-ray and neutron scattering, have confirmed the presence of a steric structural model for asphaltene and resins (Bardon *et al.*, 2006), and adsorbed resins molecules are seen to be smaller than asphaltene molecules. According to Aske *et al.* (2002), the stability of the colloidal dispersion of asphaltenes by resin molecules may be affected by temperature, pressure, and fluid composition.

Recall, the dry volume fraction of asphaltene defined in eq. (14). However, in order to account for the solvation effects that occur when resin molecules adsorb onto the surface of the asphaltene aggregates exist in a colloidal system, an effective volume fraction is defined as:

$$\varphi_{eff} = \frac{V_a+V_s}{(V_a+V_s)+(V_m-V_s)} = \frac{V_a+V_s}{V_a+V_m} \tag{33}$$

where, V_s is the volume of the resin solvation shell surrounding an asphaltene aggregate, which originally existed in the maltene, however is now attached to the surface of the asphaltene particle.

The following relationships should be noted:

$$\varphi_{eff} - \varphi = \frac{V_s}{V_a + V_m} \tag{34a}$$

$$\varphi_{eff}/\varphi - 1 = \frac{V_s}{V_a} \tag{34b}$$

$$\frac{1}{\varphi_{eff}/\varphi - 1} = \frac{V_a}{V_s} \tag{34c}$$

The process of formation of the solvation shell is now explained.

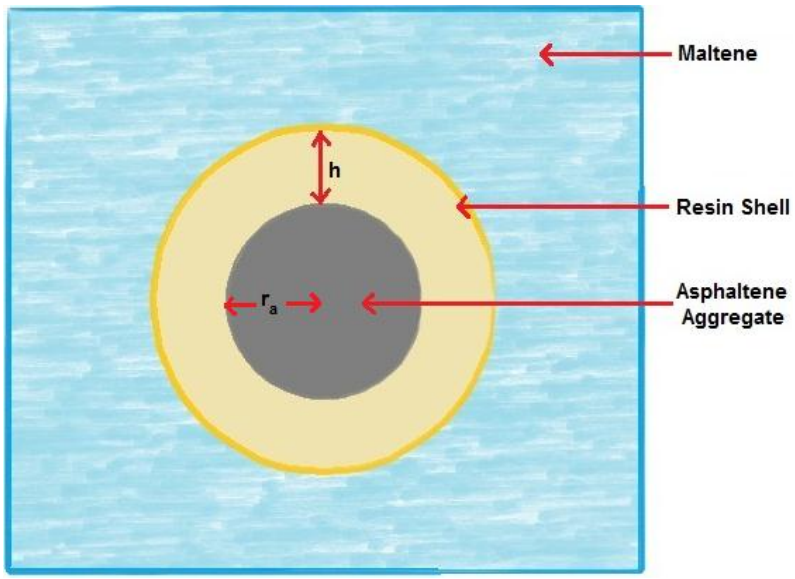

Figure 1 – Asphaltene- Resin Solvation Model showing Asphaltene Particle Radius, r_a and Solvation Shell Thickness, h

The volume of the solvation shell can be estimated as:

$$V_s = S_a . h \tag{35}$$

where S_a= surface area of the asphaltene aggregate, and h= thickness of the solvation shell around the asphaltene aggregate (see fig.1).

The asphaltene aggregate for the purpose of this model is assumed to be spherical in shape, with a radius, r_a, such that:

$$S_{asp} = 4\pi r_a^2 N_A n_a \tag{36}$$

$$V_a = 4\pi/3\, r_a^3 N_A n_a \tag{37}$$

where, N_A= Avogadro's number= 6.0221415×10^{23} and, n_a= number of moles of asphaltene aggregates.

Recall the relationship:

$$\frac{1}{\varphi_{eff}/\varphi - 1} = \frac{V_a}{V_s} = \frac{4\pi/3\, r_a^3 N_A n_a}{4\pi r_a^2 N_A n_a h} = \frac{r_a}{3h} \tag{38}$$

The ratio of the radius of the asphaltene particle to the resin shell thickness, r_a/h is then given by:

$$\frac{r_a}{h} = \frac{3}{\varphi_{eff}/\varphi - 1} \tag{39}$$

Results and Discussion

Model Validation. The following tables summarise the results for the back- calculated asphaltene volume fractions, φ_{eff}, against the asphaltene volume fractions calculated according to Luo *et al*. (2007) for each of the three colloidal viscosity models (including Einstein (1906)), at all six isotherms.

Table 1 - Volume Fraction (Luo *et al.*, 2007) versus Effective Volume Fraction - Brady (1993)

Weight Fraction, wt/wt	Volume Fraction, vol/vol (Luo *et al.*, 2007)	Effective Volume Fractions, vol/vol					
		Temperature, K					
		293.15	297.05	303.15	313.15	323.15	333.15
0.1601	0.1346	0.492	0.483	0.467	0.448	0.423	0.404
0.1502	0.1263	0.481	0.473	0.457	0.438	0.413	0.394
0.1450	0.1219	0.467	0.460	0.443	0.423	0.397	0.379
0.1402	0.1179	0.448	0.441	0.426	0.408	0.383	0.363
0.1236	0.1039	0.424	0.412	0.398	0.378	0.353	0.335
0.0998	0.0839	0.360	0.352	0.337	0.322	0.300	0.281
0.0804	0.0676	0.308	0.301	0.287	0.274	0.252	0.237
0.0613	0.0515	0.239	0.231	0.220	0.210	0.188	0.179
0.0385	0.0324	0.157	0.150	0.136	0.130	0.127	0.115
0.0196	0.0165	0.084	0.091	0.075	0.083	0.066	0.055
0.0000	0.0000	0.000	0.000	0.000	0.000	0.000	0.000

Table 2- Volume Fraction (Luo *et al.*, 2007) versus Effective Volume Fraction – Verberg et al. (1997)

Weight Fraction, wt/wt	Volume Fraction, vol/vol (Luo *et al.*, 2007)	Effective Volume Fractions, vol/vol					
		Temperature, K					
		293.15	297.05	303.15	313.15	323.15	333.15
0.1601	0.1346	0.479	0.470	0.454	0.436	0.412	0.395
0.1502	0.1263	0.467	0.460	0.444	0.426	0.403	0.386
0.1450	0.1219	0.454	0.446	0.431	0.412	0.389	0.373
0.1402	0.1179	0.435	0.428	0.414	0.398	0.376	0.360
0.1236	0.1039	0.413	0.402	0.389	0.372	0.351	0.335
0.0998	0.0839	0.356	0.350	0.337	0.324	0.305	0.289
0.0804	0.0676	0.312	0.306	0.294	0.282	0.264	0.250
0.0613	0.0515	0.252	0.245	0.235	0.226	0.205	0.196
0.0385	0.0324	0.175	0.169	0.154	0.148	0.145	0.133
0.0196	0.0165	0.100	0.107	0.090	0.098	0.079	0.067
0.0000	0.0000	0.000	0.000	0.000	0.000	0.000	0.000

Table 3 - Volume Fraction (Luo *et al.*, 2007) versus Effective Volume Fraction – Einstein (1906)

Weight Fraction, wt/wt	Volume Fraction, vol/vol (Luo *et al.*, 2007)	Effective Volume Fractions, vol/vol					
		Temperature, K					
		293.15	293.15	293.15	293.15	293.15	293.15
0.1601	0.1346	7.905	6.917	5.589	4.414	3.313	2.701
0.1502	0.1263	6.720	6.071	4.897	3.896	2.977	2.446
0.1450	0.1219	5.573	5.064	4.159	3.311	2.531	2.112
0.1402	0.1179	4.384	4.028	3.399	2.811	2.198	1.831
0.1236	0.1039	3.325	2.936	2.540	2.104	1.670	1.425
0.0998	0.0839	1.773	1.648	1.452	1.269	1.054	0.903
0.0804	0.0676	1.135	1.070	0.953	0.850	0.714	0.629
0.0613	0.0515	0.636	0.598	0.546	0.502	0.412	0.379
0.0385	0.0324	0.309	0.290	0.250	0.234	0.227	0.198
0.0196	0.0165	0.132	0.146	0.115	0.130	0.098	0.080
0.0000	0.0000	0.000	0.000	0.000	0.000	0.000	0.000

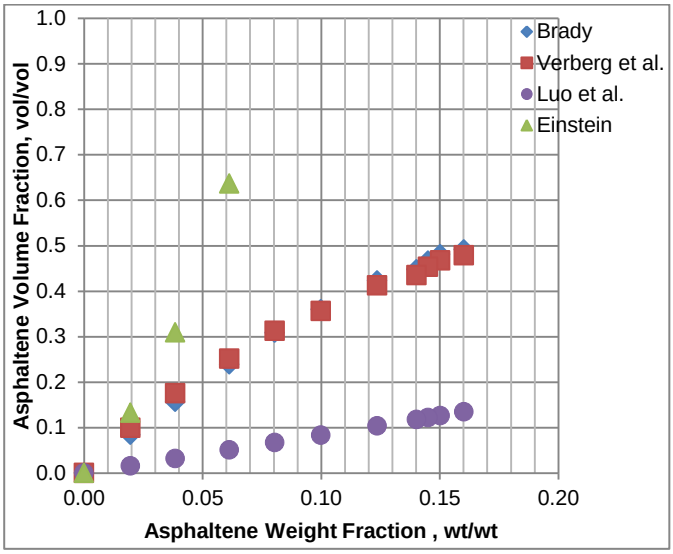

Figure 2 – Volume Fractions versus Weight Fraction at T= 293.15K

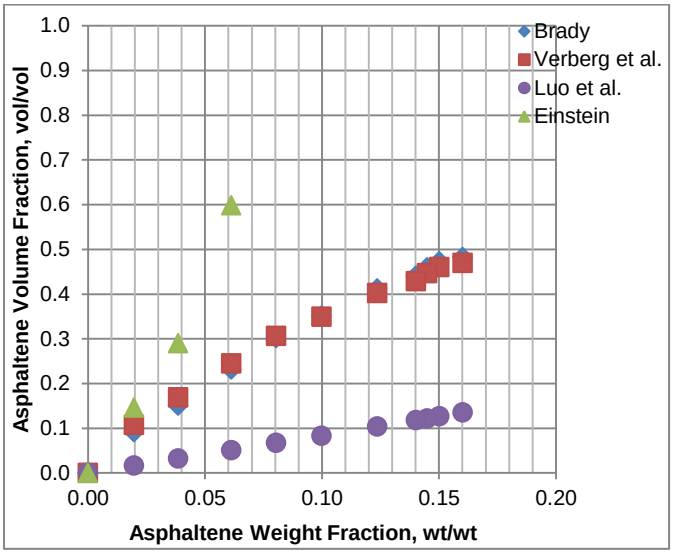

Figure 3 – Volume Fractions versus Weight Fraction at T= 297.05K

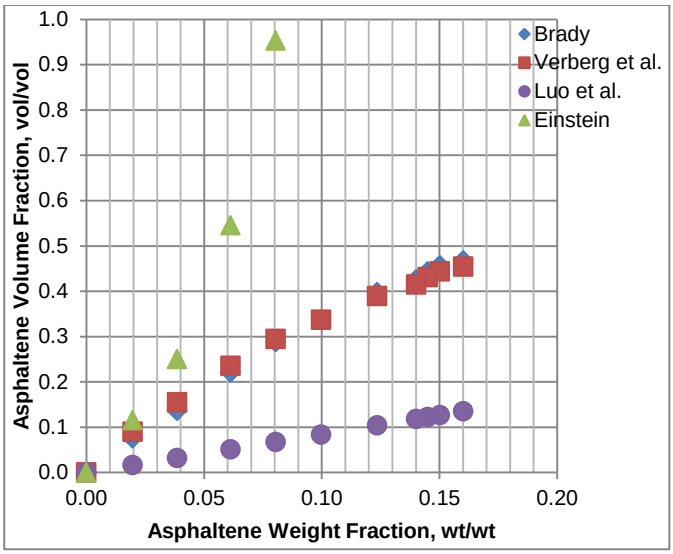

Figure 4 – Volume Fractions versus Weight Fraction at T= 303.15K

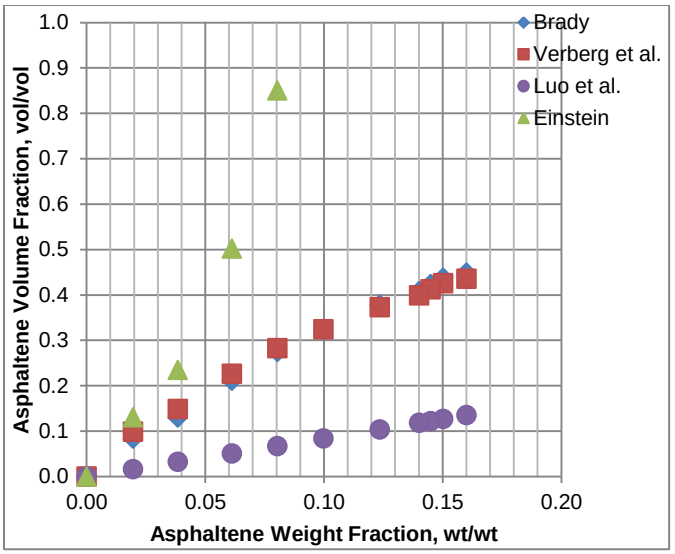

Figure 5 – Volume Fractions versus Weight Fraction at T= 313.15K

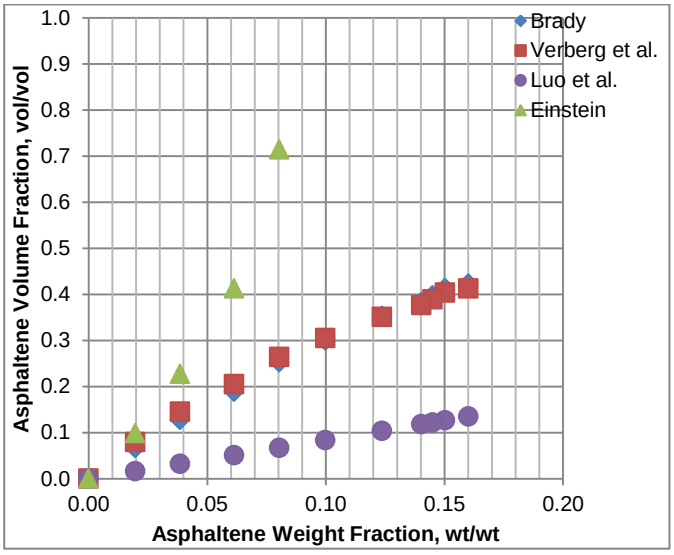

Figure 6 – Volume Fractions versus Weight Fraction at T= 323.15K

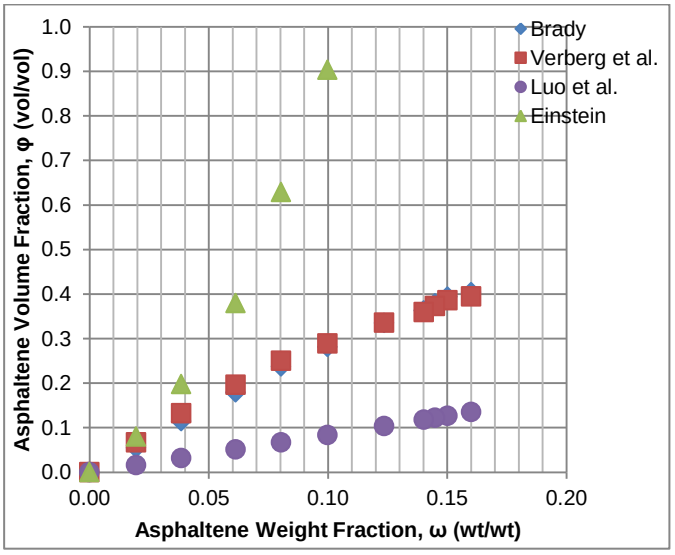

Figure 7 – Figure 6 – Volume Fractions versus Weight Fraction at T= 333.15K

The results in tables 1 to 3 are summarised in figures 2 to 7 above, showing the effective asphaltene volume, φ_{eff}, based on the three models, compared with the asphaltene volume fraction, φ, calculated according to Luo *et al.* (2007) at each isotherm. In figures 2 to 7, all values greater than 1 have been excluded for the Einstein (1906) model.

It is immediately apparent that the effective volume fractions calculated using all three colloidal viscosity models are significantly larger than the dry volume fractions calculated according to Luo *et al.* (2007).
The most noticeable difference is seen with the Einstein (1906) model, which yields effective volume fractions, an order of magnitude larger than all other three models. This behaviour is not surprising as the Einstein equation is only valid for volume fractions ≤ 2 vol%. Both Brady (1993) and Verberg *et al.* (1997) models however, yield more consistent results, and as seen in figures 2 to 7 appear to track each other relatively closely. The effective volume fractions calculated using the Brady (1993) model are seen to track the dry volume fractions according to Luo *et al.* (2007) more closely at lower asphaltene weight fractions, and deviate at higher weight fractions. This behaviour is expected as Brady (1993) predicts the viscosity model to deviate as asphaltene volume fraction approaches the close packing volume fraction, φ_{max}, due to the number of "contacting" particles in suspension tending to infinity, as particles in contact stick to each other.

Figures 8 to10 show the ratio of the effective volume fraction φ_{eff}, to the dry volume fractions, φ calculated by Luo *et al.* (2007), φ_{eff}/φ.

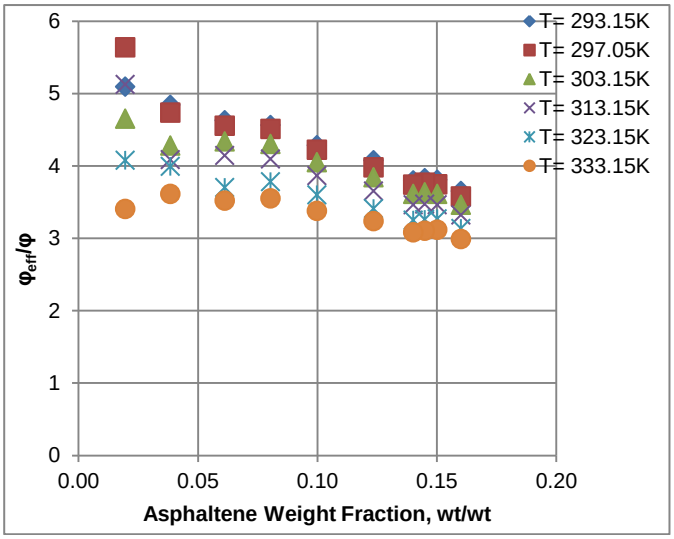

Figure 8 – Effective Volume Fraction to Dry Volume Fraction Ratio, φ_{eff}/φ vs. Weight Fraction, ω (Brady, 1993)

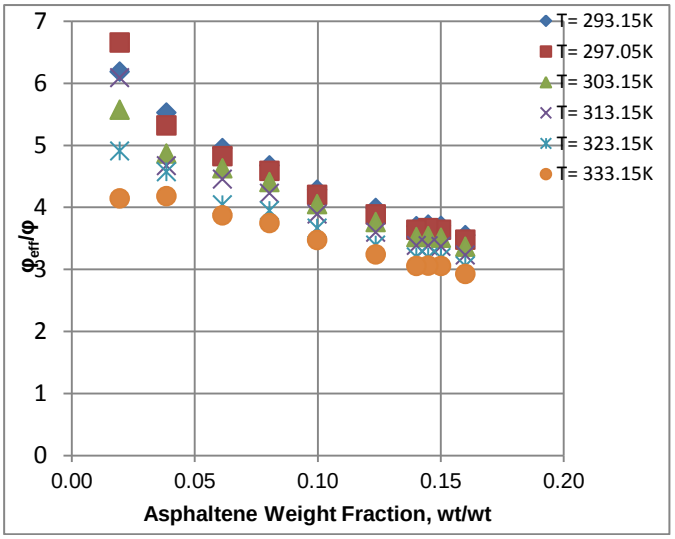

Figure 9 – Effective Volume Fraction to Dry Volume Fraction Ratio, φ_{eff}/φ vs. Weight Fraction, ω (Verberg, 1997)

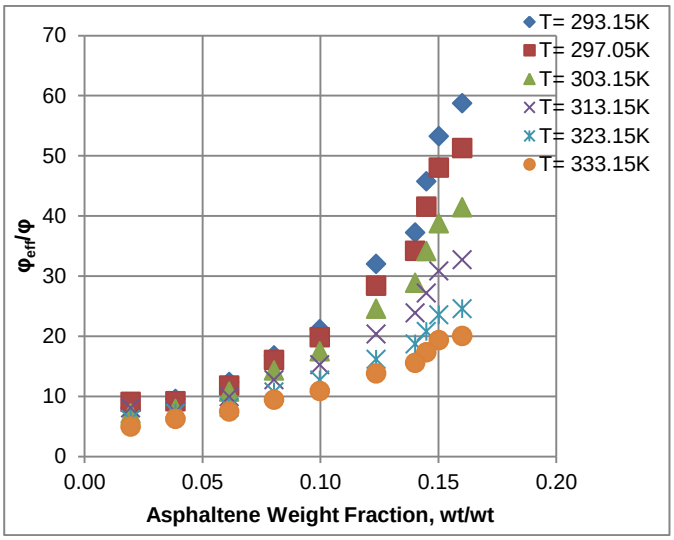

Figure 10 – Effective Volume Fraction to Dry Volume Fraction Ratio, φ_{eff}/φ vs. Weight Fraction, ω (Einstein, 1906)

From the figures above, both Brady (1993) and Verberg *et al.* (1997) models show decrease in the effective volume fraction to dry volume fractions ratio, φ_{eff}/φ as the asphaltene weight fraction increases. The Einstein (1906) model however, shows an opposite trend, with φ_{eff}/φ values in the range 5 to 60, across all isotherms. Smaller φ_{eff}/φ values at lower asphaltene content again reinforce the applicability of the Einstein (1906) model for use with only very diluted dispersions.

Due to the similarities between the Brady (1993) and Verberg et al. (1997) models, as well as their applicability at higher asphaltene concentrations (crucial for the viscosity modelling of heavy oil), all further results shown in this paper will be based on these two models.

Temperature Effects. The effects of temperature are paramount in this study. The original data set provided by Luo et al. (2007) shows an increase in temperature from 293.15 to 333.15K causes a reduction in the viscosity of the reconstituted heavy oil samples by 1 to 2 orders of magnitude, at a given asphaltene weight fraction. The effect of temperature can be described with the Arrhenius equation, based on Eyring's theory of viscosity (Bird *et al.*, 2002):

$$\mu(T) = \mu(T_0) exp\left[\frac{E_a}{R}\left(\frac{1}{T} - \frac{1}{T_0}\right)\right] \tag{40}$$

where $\mu(T)$ is the viscosity of the liquid at absolute temperature T, $\mu(T_0)$ is the viscosity of the liquid at a reference temperature T_0, E_a is the activation energy of viscous flow (J/mol) and R is the universal gas constant (J/ K mol).

As temperature increases, the liquid molecules gain thermal energy, which increases the average kinetic energy of the molecules in the liquid, overcoming cohesive intermolecular forces which allow the molecules move around freely to occupy vacant sites, allowing the heavy oil sample to flow more easily.

Effective Volume Fraction, φ_{eff}. Both tables 1 to 3 and figure 2 to 7 above, show a reduction in asphaltene effective volume fractions with an increase in temperature. Assuming the resin solvation shell model holds, where resin molecules are adsorbed to the surface of the asphaltene particle, an increase in temperature will increase the thermal energy of the resin molecules adsorbed on the outermost layer of the shell. This results in an increased kinetic energy allowing the resin molecules to vibrate about their position. Once enough thermal energy is gained, the resin molecules completely break free off the asphaltene particle, hence reducing the effective volume fraction.

Effective Volume Fraction to Dry Volume Fraction Ratio, φ_{eff}/φ. Assuming the dry volume fraction remains constant across all isotherms, a reduction in effective volume fraction with increasing temperature will result in corresponding reduction in the φ_{eff}/φ ratio. This is seen in both figures 8 and 9 above with Brady (1993) and Verberg *et al.* (1997) models.

Density Approach for Determining Dry Volume Fraction, φ. Equation (26) provides an alternative to eq. (11) according to Luo *et al.* (2007) that takes into account the change in density of maltene, ρ_m with temperature. Equation (11) assumes the density of the original oil sample, ρ_o to be constant, when it ideally should change with temperature. Equation (27) takes the density of the maltene at 298.15K, $\rho(T= 298K)$ to be the density of maltene at 297.05K (for proximity purposes), which, according to Luo *et al.* (2007) is 962 kg/m^3 (or 0.962 g/cm^3). From equation (27) a carbon number per molecule, n, is found to be approximately 221.0.
The coefficient of thermal expansion, α according to Kartsev *et al.* (1997) in eq. (28) is 6.91×10^{-4} K^{-1}.
The densities of maltene at all six experimental isotherms are then calculated using eq. (29) - the results are summarized in the table below:

Table 4- Density of Maltene, ρ_m at Different Constant Temperatures (Aasen et al.)

Temperature (K)	Density of Maltene, kg/m^3
293.15	965.4
297.05	962.8
303.15	958.8
313.15	952.1
323.15	945.5
333.15	938.8

With the density of asphaltene, ρ_a remaining constant at 1175.3 kg/m^3, asphaltene volume fraction, φ, at different constant temperatures can then be determined with eq. (26). The dry volume fractions calculated with eq. (26) at different constant temperatures showed very little difference from those calculated at a single reference temperature, T= 23.9 °C according to Luo *et al.* (2007), with maximum percentage deviation of ≈2%.

This model justifies the work done by Luo *et al.* (2007) reinforcing that over the experimental temperature range, T= 293.15 to 333.15K, the asphaltene dry volume fraction varies insignificantly with temperature.

Solvation Shell Model. Both Brady (1993) and Verberg et al. (1997) models and give the viscosity a heavy oil sample, μ as a function of both the effective volume fraction, φ_{eff} and the viscosity of maltene, μ_0:

$$\mu = \mu(\mu_0, \varphi_{eff}) \tag{41}$$

However, the only known input data to determine the heavy oil viscosity is the viscosity of maltene, μ_0, the dry asphaltene volume fraction, φ and the weight fraction of asphaltene, ω. Using the solvation model, eq. (39), the aim is to derive an expression that gives the heavy oil viscosity as a function of the known variables- i.e. asphaltene weight fraction, ω (with eq. (26), the viscosity of maltene, μ_0, and temperature, T:

$$\mu = \mu(\mu_0, \omega, T) \tag{42}$$

Asphaltene Particle Radius to Resin Shell Ratio, r_a/h – Weight Fraction, ω Relationship. Using the effective volume fractions in tables 1 and 2 for both the Brady (1993) and Verberg *et al.* (1997) models, and the dry volume fractions, φ calculated with eq. (26) (assuming the density of maltene, ρ_m stays constant across all isotherms, φ should be in agreement with Luo et al. (eq. (11)), the asphaltene particle radius to resin shell thickness ratio, r_a/h, can be calculated, at all asphaltene weight fractions, ω and across all isotherms with eq. (39).
The ratio, r_a/h, is plotted against ω, for both models, at all isotherms to give the relationships shown in the figures below:

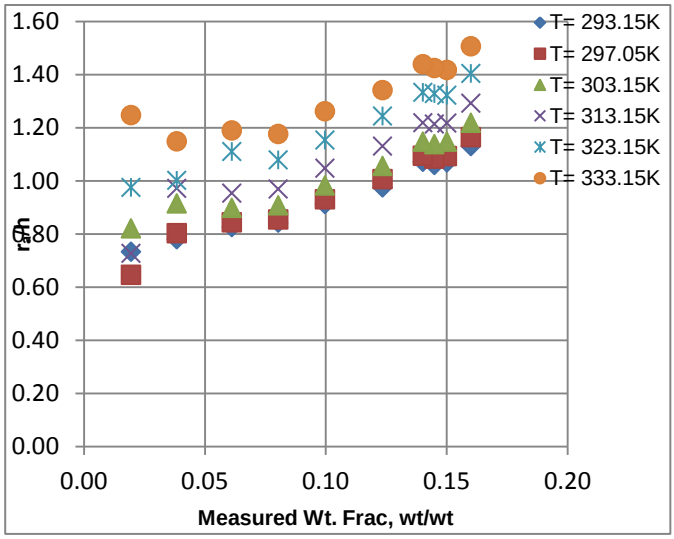

Figure 11 – Asphaltene Radius to Solvation Shell Thickness ratio, r_a/h vs. Asphaltene Weight Fraction, ω (Brady, 1993)

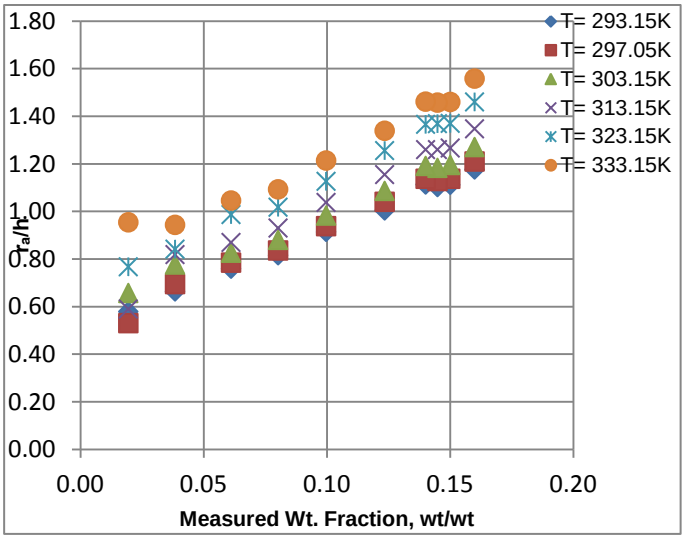

Figure 12 – Asphaltene Radius to Solvation Shell Thickness ratio, r_a/h vs. Asphaltene Weight Fraction, ω (Verberg *et al.*, 1997)

Based on the above plots, a linear relationship is observed between the asphaltene weight fraction, and the asphaltene particle radius to resin shell thickness ratio, where r_a/h generally increases as ω increases. The increase of r_a/h with ω might suggest that asphaltene particles aggregate as its concentration increases, forming particles of larger sizes. At higher temperatures, the ratio is seen to be larger than at lower temperatures. This behaviour is the result of a thinning resin shell (h reduced) at higher temperatures as the resin molecules deabsorb from the asphaltene particle surface as they gain enough thermal energy to break free. This could also be the result of asphaltene aggregates breaking up into smaller individual particle as they also gain thermal energy, causing a reduction in the overall asphaltene particle radius, r_a.
For both models, at each isotherm, a linear relationship relating ω and r_a/h, takes the form:

$$r_a/h = a\omega + b \tag{43}$$

The tables below summarise the constants *a* and *b* at all six temperatures for both Brady (1993) and Verberg *et al.* (1997) model:

Table 5 - r_a/h vs. ω Constants (Brady, 1993)

Temperature, T (K)	a	b	Maximum Percentage Deviation, Δ_{max} (%)
293.15	2.9539	0.6312	6
297.05	3.3333	0.6	9
303.13	2.5581	0.76	6
313.15	3.7551	0.6764	16
323.15	2.9798	0.8915	5
333.15	2.9686	0.9932	16

Table 6 - r_a/h vs. ω Constants (Verberg *et al.*, 1997)

Temperature, T (K)	a	b	Maximum Percentage Deviation, Δ_{max} (%)
293.15	4.2043	0.4851	3
297.05	4.2151	0.4943	9
303.13	4.4482	0.545	8
313.15	4.6507	0.5764	13
323.15	4.8882	0.6594	3
333.15	5.0481	0.7253	14

The constants are plotted against temperature to obtain a linear relationship for the constant dependence on temperature. The resulting fitting correlations are shown on the following page:

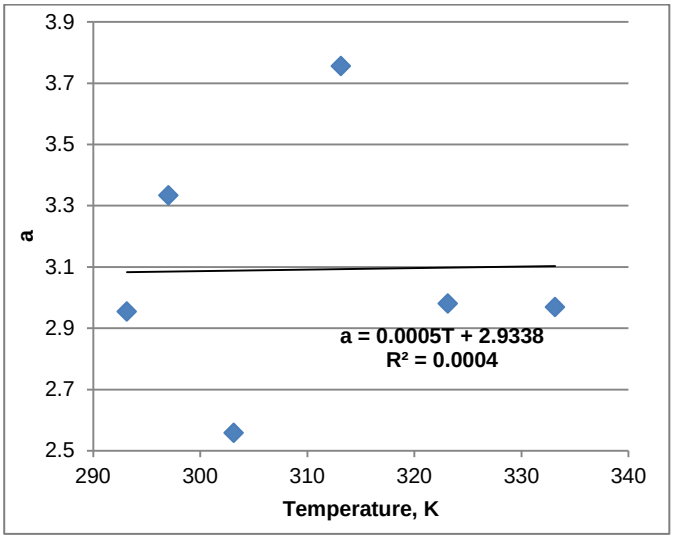

Figure 13 – Constant *a* vs. Temperature, T (Brady, 1993)

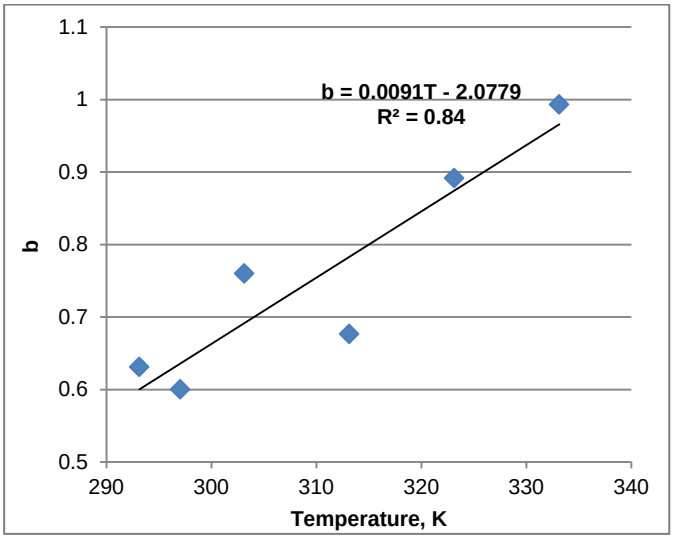

Figure 14 – Constant *b* vs. Temperature T (Brady, 1993)

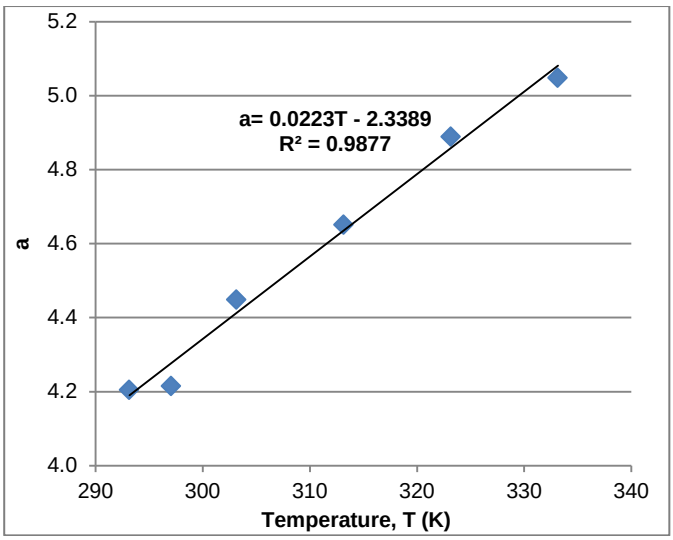

Figure 15 – Constant *a* vs. Temperature, T (Verberg *et al.*, 1997)

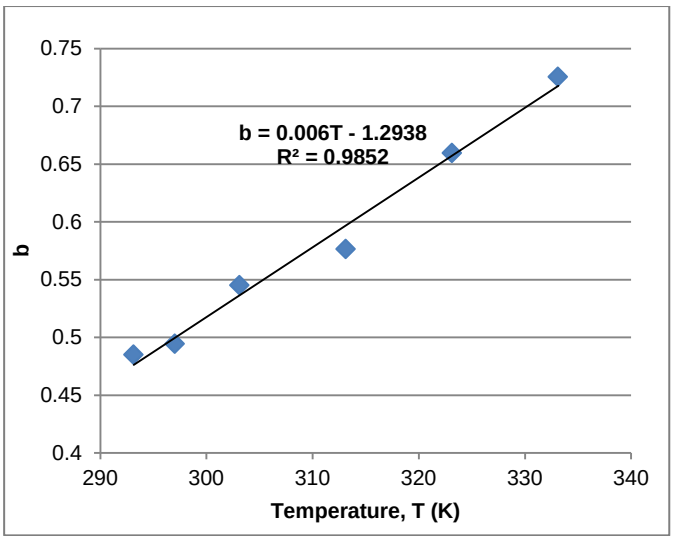

Figure 16 – Constant *b* vs. Temperature, T (Verberg *et al.*, 1997)

Brady (1993): $a = 0.0005T + 2.9338$ (44)

$b = 0.0091T - 2.0779$ (45)

Verberg *et al.* (1997): $a = 0.0223T - 2.3389$ (46)

$b = 0.006T - 1.2938$ (47)

where T is in Kelvin.

Figure 13 shows that the constant *a* is largely independent of temperature – this result however, is most likely the result of the fitting procedure used to determine the linear relationship between ω and r_d/h. The Verberg *et al.* (1997) model in figures 15 and 16 show better linearity with ω, and both constants *a* and *b* are seen to vary linearly with temperature.

Correlation of Viscosity of Asphaltene – Containing Oil. Equations (44) to (47) are used to calculate the constants *a* and *b*, for the respective model, at the desired temperature, T. Once the correct constants are obtained, the r_d/h ratio can then be determined by using the linear relationship in eq. (43) at the respective asphaltene weight fraction, ω. With the ratio r_d/h now known both the solvation model eq. (39) and eq. (26) are be combined, and with a simple rearrangement the effective asphaltene volume fraction, φ_{eff} is given as:

$$\varphi_{\text{eff}} = \left(\frac{\omega_a}{\omega_a + \frac{\rho_a}{\rho_m}(1-\omega_a)}\right)\left(1 + \frac{3\text{h}}{\text{r}_\text{a}}\right) \tag{48}$$

The effective asphaltene volume fraction, φ_{eff} can then be substituted into either Brady (1993) or Verberg *et al.* (1997) models to give the relative viscosity of the heavy oil sample at all six isotherms.

The tables 7 and 8 below summarise the percentage deviation of the relative viscosity of the heavy oil samples calculated using both Brady (1993) and Verberg *et al.* (1997) models, $\mu_{r,\,calc}$ to the measured relative viscosity provided by Luo *et al.* (2007), μ_r.

Table 7- Percentage Deviation of Calculated Relative Viscosity, $\mu_{r,\,calc}$ and Measured Relative Viscosity, μ_r at Different Constant Temperatures (Verberg et al.)

Asphaltene Weight Fraction, ω (wt/wt)	Percentage Deviation between $\mu_{r,calc}$ and μ_r at Different Constant Temperatures					
	293.15K	297.05K	303.15K	313.15K	323.15K	333.15K
0.1601	6%	4%	4%	-1%	3%	3%
0.1502	-4%	-7%	-5%	-9%	-5%	-4%
0.1450	1%	-3%	-2%	-5%	0%	-1%
0.1402	12%	8%	6%	0%	3%	4%
0.1236	-2%	-1%	-2%	-5%	-2%	-2%
0.0998	1%	-1%	-1%	-5%	-3%	-2%
0.0804	-3%	-4%	-4%	-7%	-4%	-4%
0.0613	2%	1%	1%	-2%	2%	1%
0.0385	1%	1%	4%	2%	-1%	1%
0.0196	0%	-3%	1%	-4%	0%	2%
0.0000	0%	0%	0%	0%	0%	0%

Table 8- Percentage Deviation of Calculated Relative Viscosity, $\mu_{r,\,calc}$ and Measured Relative Viscosity, μ_r at Different Constant Temperatures (Brady et al.)

Asphaltene Weight Fraction, ω (wt/wt)	Percentage Deviation between $\mu_{r,calc}$ and μ_r at Different Constant Temperatures					
	293.15K	297.05K	303.15K	313.15K	323.15K	333.15K
0.1601	30%	22%	17%	7%	10%	10%
0.1502	9%	2%	1%	-5%	-1%	0%
0.1450	10%	4%	3%	-1%	3%	3%
0.1402	20%	13%	10%	3%	6%	7%
0.1236	0%	0%	-2%	-4%	0%	0%
0.0998	1%	-1%	-1%	-5%	-2%	0%
0.0804	-1%	-3%	-3%	-6%	-3%	-2%
0.0613	4%	3%	3%	-1%	3%	2%
0.0385	4%	4%	6%	4%	1%	2%
0.0196	2%	-2%	2%	-3%	1%	3%
0.0000	0%	0%	0%	0%	0%	0%

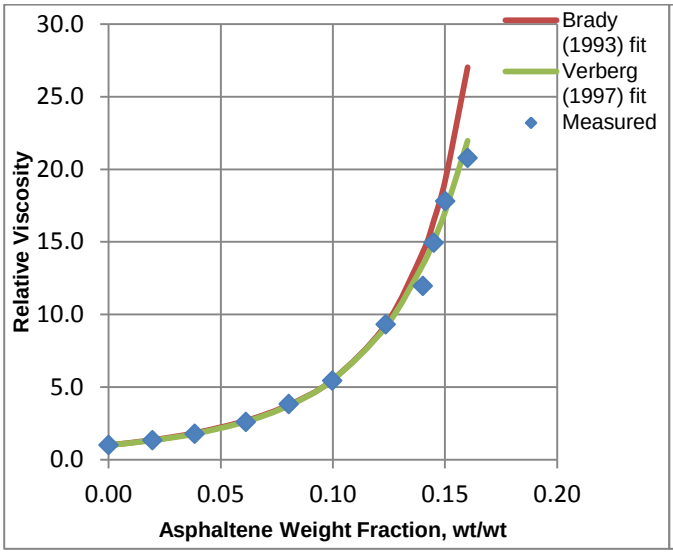

Figure 17 – Relative Viscosity vs. Weight Fraction, T= 293.15K

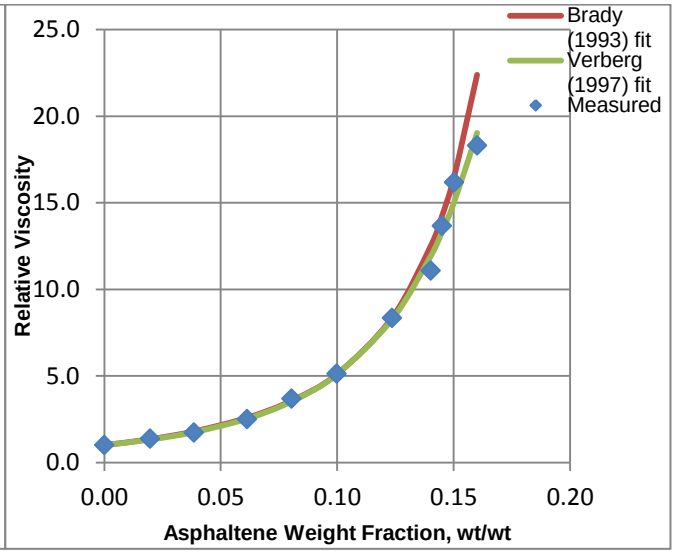

Figure 18 – Relative Viscosity vs. Weight Fraction, T= 297.05K

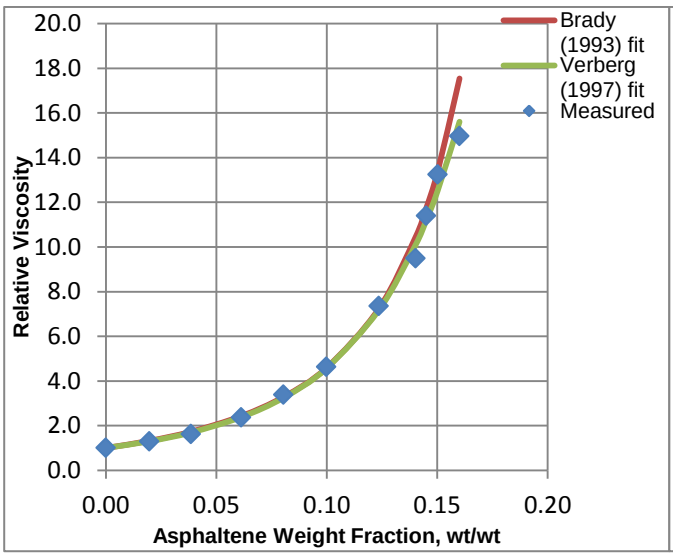

Figure 19 – Relative Viscosity vs. Weight Fraction, T= 303.15K

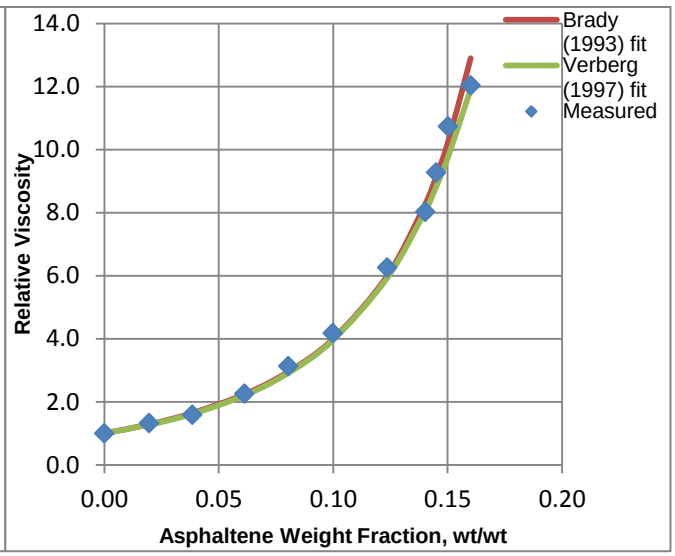

Figure 20 – Relative Viscosity vs. Weight Fraction, T= 313.15K

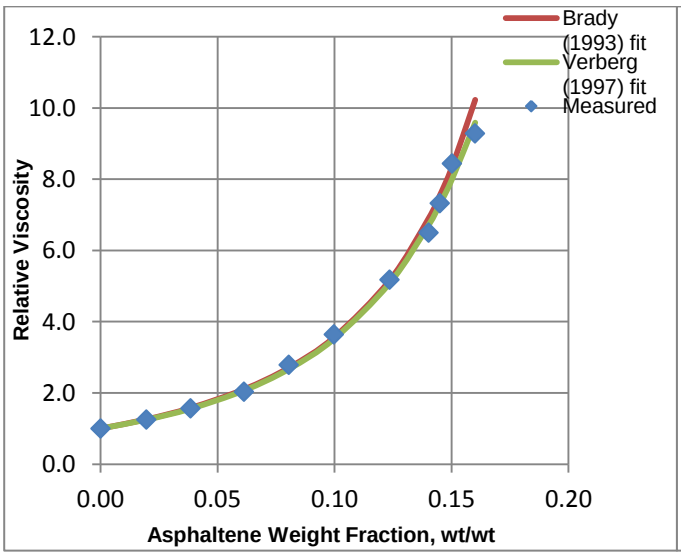

Figure 21 – Relative Viscosity vs. Weight Fraction, T= 323.15K

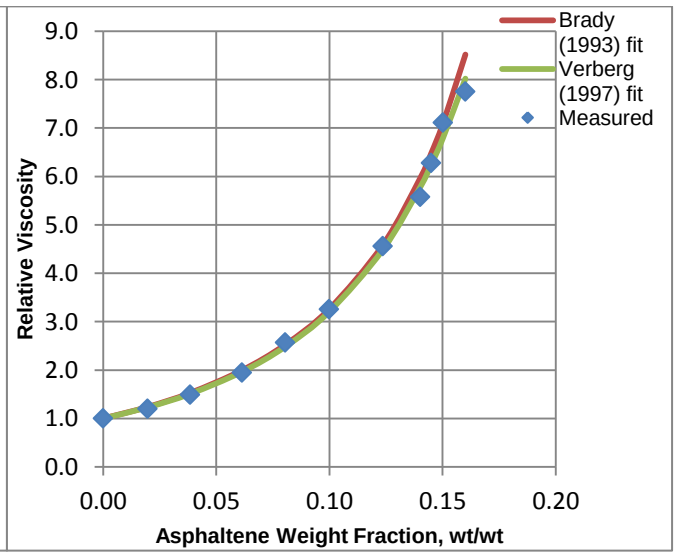

Figure 22 – Relative Viscosity vs. Weight Fraction, T= 333.15K

From table 7 and 8 and figures 17 to 22 above it is clear that the Verberg *et al.* (1997) model produces a better match to the measured relative viscosity data than the Brady (1993) model. Both models at low asphaltene weight fractions give reasonable matches to the measured relative viscosity numbers, with deviations well within the acceptable 5% error margin. According to Luo *et al.* (2007), the largest relative error in the viscosity measurements, based on an average value of three viscosity measurements was found to be 3.39%. Brookfield Engineering quotes an error of ±1.0% the cone-plate viscometer (DV-II+, Brookfield Engineering Laboratories, USA) used by Luo *et al.* (2007) in taking the viscosity measurement of the heavy oil sample. Considering all, a 5% error margin is deemed acceptable.

At higher weight fractions, the Verberg *et al.* (1997) model remains truest to the measured viscosity data, with values for relative viscosity, mostly within the accepted 5% error margin. The Brady (1993) model, however, is seen to deviate at higher asphaltene weight fractions and especially at lower temperatures. Again this behaviour is already expected as Brady (1993) predicts the viscosity to deviate as asphaltene volume fraction approaches the close packing volume fraction, φ_{max}, due to the number of "contacting" particles in suspension tending to infinity, with touching particles sticking to each other as a result of hydrodynamic lubrication forces.

Summary and Conclusion

This study took advantage of experimental data sets to develop a simple empirical model for the prediction of heavy oil viscosity, using of the viscosity of maltene, μ_0, temperature, T, and asphaltene weight fraction, ω as the input data.

Given the viscosity measurements of reconstituted Lloydminster heavy oil samples, with asphaltene weight fractions, ω, within the range 0 to 0.1601 wt/wt (Luo *et al.*, 2007), the colloidal viscosity models of Brady (1993), Verberg *et al.* (1997) and Einstein (1906) were employed to estimate the variations between the effective asphaltene volume fraction, φ_{eff} and the dry asphaltene volume fraction, φ according to Luo *et al.* (2007). It was found that all three models yielded values of effective asphaltene volume fraction, φ_{eff} significantly larger than the dry volume fractions, φ. The most noticeable difference, however, was in the φ_{eff} values from the Einstein (1906) model, which were an order of magnitude larger than the dry volume fractions. Both Brady (1993) and Verberg *et al.* (1997) models produced more consistent results for effective asphaltene volume fraction, with values that appear to track each other very well. Effective volume fractions calculated with the Brady (1993) model are found to deviate as higher asphaltene weight fractions. This behaviour is expected as Brady (1993) predicts the viscosity model to deviate as asphaltene volume fraction approaches the close packing volume fraction, φ_{max}, due to the number of "contacting" particles in suspension tending to infinity, with touching particles sticking to each other as a result of hydrodynamic lubrication forces.

In order to rationalise the disparity between the effective and dry asphaltene volume fractions, a steric structural model for the solvation of asphaltenes was explored. This model assumes asphaltene molecules become colloidal dispersions in oil due to the presence of resins and other polar molecules, which adsorb onto the surface of the asphaltene molecules, thereby increasing its overall *effective* volume fraction. The model results in an equation that gives the effective volume fraction as a function of the asphaltene weight fraction, ω, the asphaltene particle radius, r_a, and the resin shell thickness, h.

Temperature effects play a dominant role throughout this study. The data set provided (see appendix D) shows a reduction in the viscosity of the reconstituted heavy oil samples by one or two orders of magnitude as the temperature increased from 293.15 to 333.15K. An increase in temperature results in a gain in thermal energy in the liquid molecules, which gain enough kinetic energy to move about freely. The effective asphaltene volume fractions are also seen to decrease with increasing temperature in all the models. Assuming the asphaltene – resin solvation model holds, an increase in temperature will result in a rise in thermal energy of the resin molecules on the outermost layers, which will eventually break free of the asphaltene, reducing the overall effective asphaltene volume fraction.

With the effective volume fraction from the solvation model, the viscosities of the reconstituted heavy oil samples are then determined using either Brady (1993) or Verberg *et al.* (1997) models. The results are compared with measured experimental data. The Verberg (1997) model yields more accurate results overall than the Brady (1993) model, with 90% of the 66 samples showing deviations from the measured viscosities within the acceptable 5% range. The Brady (1993) model as predicted, yields less accurate viscosities at higher asphaltene effective volume fractions, and especially at lower temperatures.

Although this model is currently limited to the Lloydminster sample, with extensive experimental data, these ideas can easily be exploited to develop more robust models.

Nomenclature

E_a = activation energy of viscous flow, J/mol
h = solvation shell thickness
K = solvation constant
n_a = number of moles of asphaltene aggregates
N_A = Avogadro's number= 6.0221415×10^{23} mol^{-1}
r_a = radius of asphaltene particle
R = universal gas constant, J/ K mol
S_a = surface area of the asphaltene aggregate
T = temperature, K
T_0 = reference temperature in Arrhenius equation, K
V = volume

Greek Letters

α = coefficient of thermal expansion, K^{-1}
β = constant in coefficient of thermal expansion, eq. (26)
μ = viscosity of reconstituted heavy oil sample, m Pa.s
μ_r = measured relative viscosity, m Pa.s
$\mu_{r,\,calc}$ = calculated relative viscosity, m Pa.s
$[\mu]$ = intrinsic viscosity, m Pa.s
μ_0 = viscosity of maltene, m Pa.s
ν = shape factor
ρ = density, kg/m^3
φ = asphaltene volume fraction, vol/vol
φ_{eff} = asphaltene effective volume fraction, vol/vol
φ_{max} = maximum packing volume fraction, vol/vol
ω = asphaltene weight fraction, wt/wt
ω_{asp} = asphaltene weight fraction in original heavy oil sample= 0.1601 wt/wt

Subscripts

a = asphaltene
m = maltene
o = oil

References

Aasen, E., Rytter, E., Øye, H. A. 1990. Viscosity of n- Hydrocarbons and Their Mixtures. Ind. Eng. Chem. Res., **29**: 1635 – 1640.

Alvarez, J., and Coates, R. 2009. Heavy Oil Recovery; Cyclical Solvent Injection, CSI. Russian Oil and Gas Technologies. http://www.rogtecmagazine.com/2009/05/heavy-oil-recovery-cyclical-solvent.html.

Aske, N., Kallevik, H., Johnsen, E. E., Sjöblom, J. 2002. Asphaltene Aggregation from Crude Oils and Model Systems Studied by Higher Pressure NIR Spectroscopy. Energy & Fuels, **16**: 1287 – 1295.

Bardon, Ch., Barre, L., Espinat, D., Guille, V., Min Hui Li, Lambard, J., Ravey, J. C., Rosenberg, E., Zemb, T. 1996. The Colloidal Structure of Crude Oils and Suspensions of Asphaltenes and Resins. Fuel Science and Technology Int'l, **14 (1&2)**: 203 – 242.

Bird, R., Stewart, W., Lightfoot, E. 2002. *Transport Phenomena*. 2nd ed. John Wiley & Sons Inc., New York.

Brady, J. F. 1993. The Rheological Behaviour of Concentrated Colloidal Dispersions. J. Chem. Phys., **99**: 567 – 581.

de la Porte, J. J., Riesco, N., and Vesovic, V. 2009. Prediction of Heavy Oil Viscosity in Current Reservoir Simulators. SPE-125500 presented at the SPE/ EAGE Reservoir Characterisation and Simulation Conference, Abu Dhabi, UAE, 19 – 21 October 2009.

Dealy, J. M. 1979. Rheological Properties of Oil Sand Bitumens. Can. J. Chem. Eng. **57**: 677- 683.

Einstein, A. 1906. A New Determination of the Molecular Dimensions. Ann Phys, **19**: 289- 306.

Heavy Oil Info. 2011. http://www.heavyoilinfo.com/blog-posts/billion_bbls_6_uk.pdf.

Hernandez, J. C., Vesovic, V., Carter, N., and Lopez, E. 2002. Sensitivity of Reservoir Simulations to Uncertainties in Viscosity. SPE-75227 presented at the SPE/DOE Improved Oil Recovery Symposium, Tulsa, Oklahoma, 13 – 17 April 2002.

Heyes, D. M., and Sugurgeirsson, H. 2004. The Newtonian Viscosity of Concentrated Stabilised Dispersions: Comparisons with the Hard Sphere Fluid. J. Rheol. **48(1)**: 223 – 248.

Hiemenz, P. C. and Rajagopalan, R. 1997. *Principles of Colloid and Surface Chemistry*, 3rd ed., Marcel Dekker Inc., New York.

Hirschberg, A. 1984. The Role of Asphaltenes in Compositional Grading of a Reservoir's Fluid Column. SPE 13171.

Kartsev, V. N., Zabelin, V. A., Andryuschenko, N. A. 1977. Temperature Dependence of the Density of Liquid n-Alkanes. Russ. J. Phys. Chem. **51**: 1563 – 1564.

Li, K., Arnett, R. L., Epstein, M. B., Ries, R. B., Bitler, L. P., Lynch, J. M., Rossini, F. D. 1956. Correlation of Physcial Properties of Normal Alkyl Series of Compounds. J. Phys. Chem., **60**: 1400- 1406.

Luo, P., Gu, Y., 2007. Effects of asphaltene Content on the Heavy Oil Viscosity at Different Temperatures. Fuel, **86**: 1069- 1078.

Mack, C. 1932. Colloid Chemistry of Asphalts. J. Phys. Chem. **36**: 2901- 2914.

Mooney, M. 1951. The Viscosity of a Concentrated Suspension of Spherical Particles. J. Colloid Sci., **6**: 162 – 170.

Nellensteyn, F.J. 1931. Chem. Weekblad, **28**: 313.

Pal, R. and Rhodes, E. 1989. Viscosity/ Concentration Relationships for Emulsions. J. Rheol., **33**: 1021- 1045.

Pfeiffer, J. P. and Saal, R. N. J. 1940. J. Phys. Chem., **44**: 139.

Sherman, P. 1983. *Encyclopedia of Emulsion Technology*. Marcel Dekker Inc., New York.

Sheu, E. Y. and Mullins, O. C. 1995. *Asphaltenes: Fundamentals and Applications*. New York: Plenum Press.

Speight, J. G. 1991. *Chemistry and Technology of Petroleum*. Marcel Dekker Inc., New York.

Verberg, R., de Schepper, I. M., and Cohen, E. G. D. 1997. Viscosity of Colloidal Suspensions. Phys. Rev. E, **55**: 3143 – 3158.

Appendix

Appendix A – Literature Reviews

Fuel 86 1069 – 1078 (2007)

Effects of Asphaltene Content on the Heavy Oil Viscosity at Different Temperatures

Authors: Luo, P., Gu, Y.

Contribution: Understanding of the behavior of the viscosity of heavy oil with varying asphaltene content and at different temperatures. Provide objective function for for two- parameter search for solving Pal- Rhodes and Mooney equations for the viscosity of colloidal suspensions.

Objective: To measure viscosities of eleven reconstituted heavy oil samples with different asphaltene contents, at six different constant temperatures. Find solvation constant, shape factor, intrinsic viscosity and maximum packing volume fraction via non- linear regression, using experimental data- measured relative viscosity μ_r and asphaltene volume fraction, φ data, based on heavy oil sample from Lloydminster, Canada.

Methodology: Standard ASTM D2007 method used to prepare reconstituted heavy oil samples of which viscosity is measured at atmospheric pressure and different constant temperatures using a cone plate viscometer. Presents a computational two-parameter to determine unknown parameters in Pal- Rhodes (Pal *et al.*, 1989) and Mooney (1951) equations by proposing an objective function to quantify the overall discrepancy between the theoretically calculated relative viscosity, μ_{rci} from the generalised Pal- Rhodes and Mooney equations, using speculative values for the unknown parameters, and the experimentally measures relative viscosity, μ_{rmi} at the same dry volume fraction φ_i of the dispersed asphaltene particles, i= 1, 2, ..., n; where n represents the number of the reconstituted heavy oil samples with different asphaltene volume fractions tested at the same temperature. Use Arrhenius equation to model viscosity dependence on temperature.

Conclusions: Heavy oil viscosity increases dramatically with high asphaltene content due to strong interactions among asphaltene particles. Pal- Rhodes paremeters, the solvation contant, K and the shape factor, ν, indicates significant solvation of the asphaltene particles in maltene as well as a non- sphericity, respectively. The intrinsic viscosity [μ] obtained using the Mooney equation agrees with [μ] = Kν. Maximum packing volume, φ_{max} is seen to increase with temperature, as effective volue fractions, φ_{eff} decrease due to resin desorption.

Comments: Finely describes effects of asphaltene on heavy oil viscosity. Provides and extensive data set, over a reasonable range of temperatures.

Physical Review E, Volume 55, Number 3 (1997)

Viscosity of Colloidal Suspensions

Authors: Verberg, R., de Schepper, I. M., Cohen, E. G. D.

Contribution: A simple expression for the Newtonian viscosity $\mu_s(\varphi)$ of neutral monodisperse hard- sphere colloidal suspensions is presented.

Objective: Provides simple expression for the Newtonian viscosity $\mu_s(\varphi)$ of neutral monodisperse hard- sphere colloidal suspensions as a function of volume fraction of the solute over the entire fluid range i.e. for volume fractions $0<\varphi<0.55$.

Methodology: Uses a linearised solution of the Smoluchowski equation, using a Padé approximation of $\mu_S(\varphi)$ for use for all $0<\varphi<0.55$ to produce a semi- empirical expression that describes the radial distribution for a hard- sphere colloidal suspension using the Carnahan- Starling approximation.

Conclusions: Expression for the Newtonian viscosity $\mu_s(\varphi)$ of neutral monodisperse hard- sphere colloidal suspensions covers a wide range of volume fractions $0<\varphi<0.55$ within a relative accuracy of less than 0.25%.

Comments: Provides rigid expression for modelling viscosity of colloidal suspensions to a reasonable accuracy, without multiple parameters such as solvation constants and shape factors.

J. Chem. Phys., Vol. 99, No. 1 (1993)

Rheological Behavior of Colloidal Dispersions

Author: Brady, J. F.

Contribution: Presents an expression for the Newtonian viscosity of a hard sphere colloidal dispersion

Objective: This paper presents a simple model for the rheological behavior of concentrated colloidal dispersions, including viscosity effects. Aims to capture macroscopic stresses for a suspension of Brownian hard spheres in describing rheological properties of hard- sphere colloidal dispersions.

Methodology: Studies the two main contributors to macroscopic stress in a suspension of Brownian hard spheres, looking at both the hydrodynamic stress (responsible for the high frequency dynamic viscosity) and Brownian stress (responsible for the viscoelastic behavior of the colloidal dispersion) as well as other contributory effects such as inter-particle forces.

Conclusions: With the model developed, the viscosity diverges at random close packing as the amount of "contacting" particles tends to infinity and short time self- diffusivity effects disappear as particles in contact stick to each other as a result of hydrodynamic lubrication forces.

Comments: Provides a rigid model for the viscosity of colloidal suspensions, effectively capturing the effects of macroscopic stresses. The viscosity predicted by the model however, diverges at close random packing volumes.

J. Rheol. 48(1), 223- 248 (2004)

The Newtonian Viscosity of Concentrated Stabilized Dispersions: Comparisons with the Hard Sphere Fluid

Authors: Heyes, D. M., Sigurgeirsson, H.

Contribution: Provides a good review of essential expressions for the viscosity of concentrated stabilized colloidal dispersions.

Methodology: Presents a current appraisal of viscosity and self- diffusion coefficient data of hard- sphere fluids and so called hard- sphere colloids using recent simulation data and those of many experimental and theoretical studies (Heyes *et al.*, 2003).

Conclusions: Heyes *et al.*, find that hard- sphere fluids and colloidal liquids behave in a similar way with packing fraction when scaled by their respective limiting viscosities at infinite dilution- an expected behavior as high packing leads to enhancement in viscosity.

Comments: A good review of colloidal viscosity models integrated into a single paper, with adequate background provided on the models, shortcomings and advantages.

Energy & Fuels, 16, 1287 – 1295 (2002)

Asphaltene Aggregation from Crude Oils and Model Systems Studied by High- Pressure NIR Spectroscopy

Authors: Aske, N., Kallevik, H., Johnsen, E.E., Sjöblom, J.

Contribution: Provides simple insight into behaviour of resins and other polar components in oil in relation to asphaltene molecules.

Methodology: Studies aggregation of asphaltenes by pressure depletion in both live crude oil and model systems of asphaltenes in toluene/ pentane solvents using high- pressure near- infrared spectroscopy along with other multivariate analytical techniques to determine the onset of asphaltene aggregation.

Comments: Provides simple insight into behaviour of resins and other polar components in oil in relation to asphaltene molecules.

Asphaltenes: Fundamentals and Applications, Plenum Press (1995)

Colloidal Properties of Asphaltenes in Organic Solvents

Authors: Sheu, E.Y., Storm, D. A.

Contribution: Provides introduction into asphaltenes as a component of petroleum liquids- its physical and chemical properties.

Methodology: Provides introduction into asphaltenes as a component of petroleum liquids- its physical and chemical properties. Introduces asphaltene micellization mechanism and micellar structure, surface tension properties, rheological measurements including viscosity – with Ratawi crude viscosity measurements making up the experimental data. Discusses effect of temperature and asphaltene polydispersity in Small Angle Neutron Scattering (SANS) analysis.

Conclusions: Reinforces the importance of the colloidal concept of asphaltenes in solution introduced by Nellensteyn *et al.* (1930) from which the peptized asphaltene micellar model is proposed by Pfeiffer *et al.* (1940). Better understanding of asphaltenes through the use of state-of–the-art equipment such as SANS. Asphaltene is found to exhibit similar physical properties to surfactant systems (Sheu *et al.*, 1995)

Comments: Provides simple insight into asphaltenes as a whole, including physical and chemical properties. Paper summarizes work done from early 20^{th} century till 1995, to unravel the complex asphaltene molecule.

Appendix B – Critical Milestones Table

Table B1- Milestones in the Viscosity of Asphaltene Containing Oil

Paper	Year of Publication	Title	Authors	Contribution
Journal of Colloid Science, 6: 162 – 170	1951	"The Viscosity of a Concentrated Suspension of Spherical Particles"	M. Mooney	Expands on Einstein's work on viscosity, formulating a semi-empirical equation for spherical particles in a suspension of finite concentration.
Journal of Rheology, 33: 1021- 1045	1989	"Viscosity/ Concentration Relationships for Emulsions"	R. Pal, E. Rhodes	Develops a viscosity/ concentration equation for non- Newtonian emulsions considering the effects of hydration and flocculation of dispersed particles.
Journal of Chemical Physics, 99: 567 – 581	1993	"Rheological Behavior of Colloidal Dispersions"	J.F. Brady	Presents a simple model for the rheological behaviour of concentrated colloidal dispersions, including viscosity effects. Studies the two main contributors to macroscopic stress in a suspension of Brownian hard spheres- the hydrodynamic stress (responsible for the high frequency dynamic viscosity) and Brownian stress (responsible for the viscoelastic behaviour of the colloidal dispersion), as well as other contributory effects such as inter-particle forces
Asphaltenes: Fundamentals and Applications (Plenum Press)	1995	"Colloidal Properties of Asphaltenes in Organic Solvents"	E. Y. Sheu, D. A. Storm	Provides a simple introduction into asphaltenes as a component of petroleum liquids, and its physical and chemical properties. Introduces asphaltene micellization mechanism and micellar structure, surface tension properties, rheological measurements including viscosity – with Ratawi crude viscosity measurements making up the experimental data. Reinforces the importance of the colloidal concept of asphaltenes in solution introduced by Nellensteyn *et al.* (1930) from which the peptized asphaltene micellar model is proposed by Pfeiffer *et al.* (1940). Better understanding of asphaltenes through the use of state-of–the-art equipment such as SANS. Asphaltene is found to exhibit similar physical properties to surfactant systems
Fuel Science and Technology Int'l, 14 (1&2): 203 – 242	1996	"The Colloidal Structure of Crude Oils and Suspensions of Asphaltenes and Resins"	Ch. Bardon et al.	Provides clear understanding of colloidal macrostructure of heavy petroleum products and complex fractions. Insight into physical structure of asphaltenes and resins, showing resin molecules are smaller than asphaltene molecules.
Physical Review E, 55: 3143 – 3158	1997	"Viscosity of Colloidal Suspensions"	R. Verberg, I. M. Schepper, E. G. D. Cohen	Uses a linearised solution of the Smoluchowski equation, using a Padé approximation of $\mu_S(\varphi)$ for use for all $0<\varphi<0.55$ to produce a semi- empirical expression that describes the radial distribution for a hard- sphere colloidal suspension using the Carnahan- Starling approximation, within a relative accuracy of less than 0.25%.
Energy & Fuels, 16, 1287 – 1295	2002	"Asphaltene Aggregation from Crude Oils and Model Systems Studied by High-Pressure NIR Spectroscopy"	N. Aske *et al.*	Studies aggregation of asphaltenes by pressure depletion in both live crude oil and model systems of asphaltenes in toluene/ pentane solvents using high- pressure near- infrared spectroscopy along with other multivariate analytical techniques to determine the onset of asphaltene aggregation.
Journal of Rheology, 48(1): 223 – 248	2004	"The Newtonian Viscosity of Concentrated Stabilized Dispersions: Comparisons with the Hard Sphere Fluid"	D. M. Heyes, H. Sigurgeirsson	Presents a current appraisal of viscosity and self-diffusion coefficient data of hard- sphere fluids and so called hard- sphere colloids using recent simulation data and those of many experimental and theoretical studies. Finds similarities in behavior of hard- sphere fluids and colloidal liquids with regards to packing fraction when scaled by their respective limiting viscosities at infinite dilution- an expected behavior as high packing leads to enhancement in viscosity.
FUEL, 86 1069 – 1078	2006	"Effects of Asphaltene Content	P. Luo, Y. Gu	Study presenting simple and practical method for analysing the complex heavy oil with the dispersed

	on Heavy Oil Viscosity at Different Temperatures"	asphaltene particles by measuring its viscosity versus its asphaltene content at different constant temperatures. Presents a computational two-parameter to determine unknown parameters in Pal- Rhodes (Pal *et al.*, 1989) and Mooney (1951) equations by proposing an objective function to quantify the overall discrepancy between the theoretically calculated relative viscosity, μ_{rci} from the generalised Pal- Rhodes and Mooney equations, using speculative values for the unknown parameters, and the experimentally measures relative viscosity, μ_{rmi} at the same dry asphaltene volume fraction φ.

Appendix C – Computer Programs

Microsoft Excel is the only program used in modelling the viscosity of the colloidal suspensions.

In the case of complex equations including terms with multiple powers, such as the Verberg et al. (1997) equation:

$$\mu_S(\phi) = \mu_0\chi(\phi)\left[1 + \frac{1.44\phi^2\chi(\phi)^2}{1-0.1241\phi+10.46\phi^2}\right] \quad \text{(C-1)}$$

where μ_s is the viscosity of the colloidal dispersion, μ_o is the viscosity of the continuous phase, and χ(φ) is defined as:

$$\chi(\phi) = \frac{1-0.5\phi}{(1-\phi)^3} \quad \text{(C-2)}$$

The volume fraction, φ is determined by entering the entire equation into an excel cell and using the 'solver' function to equate the contents of the cell containing the equation to the desired value, from which a value for φ is calculated.

Appendix D – Sample Data (Luo *et al.*, 2007)

Compositional Analysis Results of the Original Crude Heavy Oil.

Table D1- Compositional Analysis Results of the Original Crude Heavy Oil (ω_{asp}= 16.01 wt.%, *n*-pentane insoluble) (Luo *et al.*, 2007)

Carbon Number	wt.%	Carbon Number	wt.%	Carbon Number	wt.%
C_1	0.00	C_{18}	2.08	C_{35}	1.47
C_2	0.00	C_{19}	2.13	C_{36}	1.40
C_3	0.00	C_{20}	1.87	C_{37}	0.87
C_4	0.00	C_{21}	2.28	C_{38}	0.85
C_5	0.00	C_{22}	1.50	C_{39}	1.35
C_6	0.00	C_{23}	2.24	C_{40}	1.23
C_7	0.00	C_{24}	2.08	C_{41}	0.62
C_8	0.00	C_{25}	1.66	C_{42}	0.61
C_9	0.00	C_{26}	1.56	C_{43}	1.10
C_{10}	0.00	C_{27}	1.80	C_{44}	0.80
C_{11}	0.00	C_{28}	1.85	C_{45}	0.80
C_{12}	0.86	C_{29}	1.56	C_{46}	0.57
C_{13}	1.14	C_{30}	1.50	C_{47}	0.72
C_{14}	1.33	C_{31}	1.93	C_{48}	0.72
C_{15}	1.74	C_{32}	1.78	C_{49}	0.68
C_{16}	1.75	C_{33}	1.04	C_{50}	47.50
C_{17}	2.01	C_{34}	1.02	**Total**	**100.00**

Measured Viscosities of the Reconstituted Heavy Oil Samples versus Asphaltene Content.

Table D2- Asphaltene Volume Fraction versus Measured Viscosity of the Reconstituted Heavy Oil Samples at Different Constant Temperatures

Weight Fraction wt/wt	Volume Fraction, vol/vol	Measured Viscosity of Reconstituted Heavy Oil Samples (mPa.s)					
		Temperature, K					
		293.15K	297.05K	303.15K	313.15K	323.15K	333.15K
0.1601	0.1346	53672.0	32323.0	15228.0	5187.0	2032.0	920.2
0.1502	0.1263	46010.0	28586.0	13468.0	4629.0	1848.0	844.5
0.1450	0.1219	38601.0	24137.0	11591.0	3999.0	1604.0	745.5
0.1402	0.1179	30916.0	19559.0	9658.0	3460.0	1422.0	662.0
0.1236	0.1039	24073.0	14738.0	7474.0	2698.0	1133.0	541.6
0.0998	0.0839	14042.0	9047.0	4708.0	1798.0	795.9	386.8
0.0804	0.0676	9917.0	6494.0	3440.0	1347.0	609.6	305.3
0.0613	0.0515	6698.0	4410.0	2404.0	971.6	444.6	231.3
0.0385	0.0324	4582.0	3048.0	1653.0	683.4	343.1	177.4
0.0196	0.0165	3441.0	2412.0	1310.0	570.8	272.8	142.4
0	0	2585.0	1767.0	1017.0	431.0	218.9	118.7

Relative Viscosities at Different Constant Temperatures. The relative viscosities used to determine the calculated volume fractions, φ, using the three colloidal viscosity models are calculated based on the viscosities shown in Table 1, in the main body of this paper.

The relative viscosity, μ_r is defined as the ratio of the viscosity of the solution, μ to the viscosity of the solvent or maltene, μ_o. The maltene viscosity is the deasphalted oil viscosity, which in table 1, is equivalent to a heavy oil sample with a asphaltene weight percent, ω= 0 wt.% (or volume percent, φ= 0 vol.%).

Therefore taking the T= 20 °C isotherm in table 1, the relative viscosity for a heavy oil sample with an asphaltene weight fraction ω= 0.1601 wt/wt is:

$$\mu_r = \frac{\mu(\omega=0.1601\frac{wt}{wt})}{\mu(\omega=0\frac{wt}{wt})} = \frac{53\ 672.0}{2585.0} = 20.76 \qquad \text{(D-1)}$$

Table D3- Asphaltene Volume Fraction versus Relative Viscosity of the Reconstituted Heavy Oil Samples at Different Constant Temperatures

Weight Fraction wt/wt	Volume Fraction, vol/vol	Relative Viscosity of Reconstituted Heavy Oil Samples (mPa.s)					
		Temperature, K					
		293.15K	297.05K	303.15K	313.15K	323.15K	333.15K
0.1601	0.1346	20.763	18.293	14.973	12.035	9.283	7.752
0.1502	0.1263	17.799	16.178	13.243	10.740	8.442	7.115
0.1450	0.1219	14.933	13.660	11.397	9.278	7.328	6.281
0.1402	0.1179	11.960	11.069	9.497	8.028	6.496	5.577
0.1236	0.1039	9.313	8.341	7.349	6.260	5.176	4.563
0.0998	0.0839	5.432	5.120	4.629	4.172	3.636	3.259
0.0804	0.0676	3.836	3.675	3.382	3.125	2.785	2.572
0.0613	0.0515	2.591	2.496	2.364	2.254	2.031	1.949
0.0385	0.0324	1.773	1.725	1.625	1.586	1.567	1.495
0.0196	0.0165	1.331	1.365	1.288	1.324	1.246	1.200
0	0	1.000	1.000	1.000	1.000	1.000	1.000

Appendix E – Calculations and Results

Percentage Deviation between Effective Volume Fractions, φ_{eff} and Dry Volume Fractions, φ. The percentage deviation is calculated using the equation below:

$$\frac{\varphi_{eff}-\varphi}{\varphi} = \%error \tag{E-1}$$

Figures E-1 to E-3 show the percentage deviations for all three models and at all six isotherms.

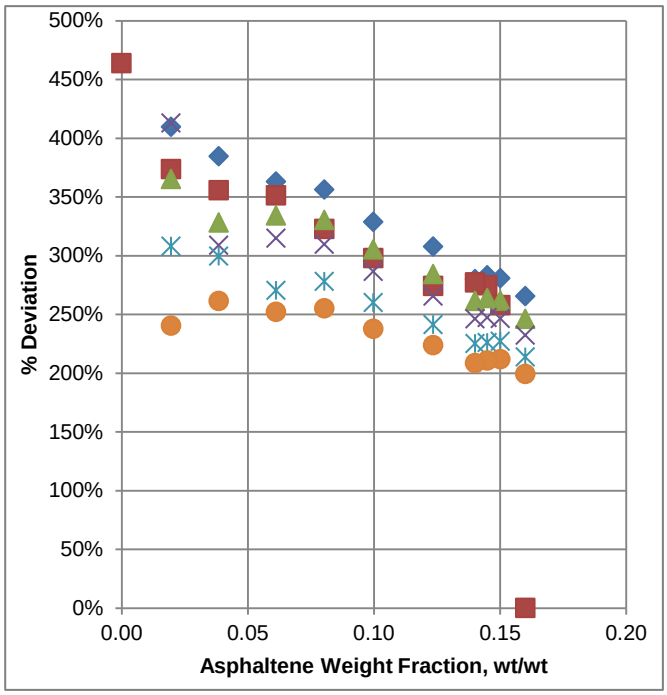

Figure E-1 – Discrepancy between φ_{eff} and φ at all isotherms (Brady, 1993)

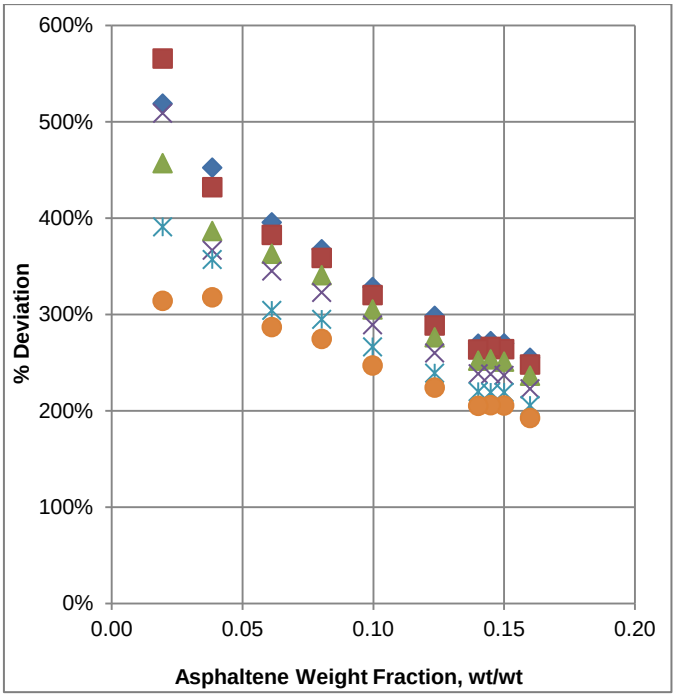

Figure E-2 – Discrepancy between φ_{eff} and φ at all isotherms (Verberg *et al.*, 1997)

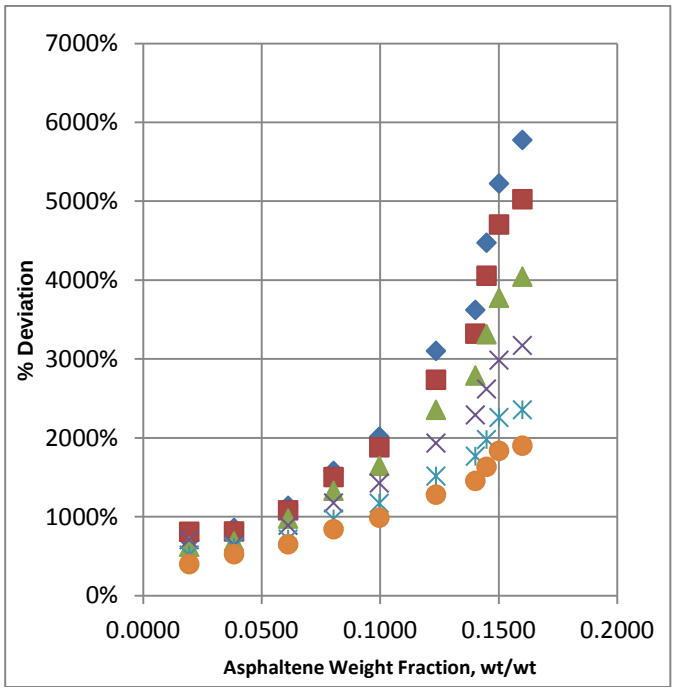

Figure E-3 – Discrepancy between φ_{eff} and φ at all isotherms (Einstein, 1906)

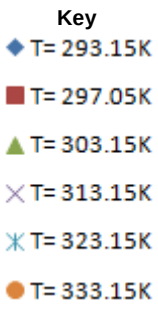

Asphaltene Particle Radius to Solvation Shell Thickness Ratio, r_a/h at Different Constant Isotherms.

Table E1- Asphaltene Particle Radius to Solvation Shell Thickness Ratio, r_a/h at Different Constant Temperatures (Brady, 1993)

Weight Fraction, ω (wt/wt)	Asphaltene Particle Radius to Solvation Shell Thickness Ratio, r_a/h					
	293.15K	297.05K	303.15K	313.15K	323.15K	333.15K
0.1601	1.13	1.16	1.22	1.29	1.40	1.51
0.1502	1.07	1.09	1.15	1.22	1.32	1.42
0.1450	1.06	1.08	1.14	1.21	1.33	1.42
0.1402	1.07	1.09	1.15	1.22	1.33	1.44
0.1236	0.98	1.01	1.06	1.13	1.24	1.34
0.0998	0.91	0.93	0.98	1.05	1.15	1.26
0.0804	0.84	0.85	0.91	0.97	1.08	1.18
0.0613	0.83	0.84	0.90	0.95	1.11	1.19
0.0385	0.78	0.80	0.91	0.97	1.00	1.15
0.0196	0.73	0.65	0.82	0.73	0.97	1.25
0.0000	1.13	1.16	1.22	1.29	1.40	1.51

Table E2- Asphaltene Particle Radius to Solvation Shell Thickness Ratio, r_a/h at Different Constant Temperatures (Verberg et al., 1997)

Weight Fraction, ω (wt/wt)	Asphaltene Particle Radius to Solvation Shell Thickness Ratio, r_a/h					
	293.15K	297.05K	303.15K	313.15K	323.15K	333.15K
0.1601	1.18	1.21	1.27	1.35	1.46	1.56
0.1502	1.11	1.14	1.19	1.27	1.37	1.46
0.1450	1.10	1.13	1.18	1.26	1.37	1.46
0.1402	1.11	1.14	1.19	1.26	1.37	1.46
0.1236	1.00	1.04	1.09	1.15	1.26	1.34
0.0998	0.91	0.94	0.98	1.04	1.13	1.21
0.0804	0.82	0.84	0.88	0.93	1.02	1.09
0.0613	0.76	0.78	0.83	0.87	0.99	1.05
0.0385	0.66	0.69	0.78	0.82	0.84	0.94
0.0196	0.58	0.53	0.66	0.59	0.77	0.95
0.0000	-	-	-	-	-	-